TOMSK POLYTECHNIC UNIVERSITY — ТОМСКИЙ ПОЛИТЕХНИЧЕСКИЙ УНИВЕРСИТЕТ

Министерство науки и высшего образования Российской Федерации
федеральное государственное автономное
образовательное учреждение высшего образования
«Национальный исследовательский Томский политехнический университет» (ТПУ)

Инженерная школа ядерных технологий
Направление подготовки 14.04.02 Ядерные физика и технологии
Отделение ядерно-топливного цикла

МАГИСТЕРСКАЯ ДИССЕРТАЦИЯ

Тема работы
Оптическая диагностика пучков современных электронных ускорителей

УДК - 621.384.6:681.784.8

Студент

Группа	ФИО	Подпись	Дата
0АМ9М	Гусвицкий Тодор		

Руководитель ВКР

Должность	ФИО	Ученая степень, звание	Подпись	Дата
Профессор ИШФВП	Потылицын Александр Петрович	д. ф.-м. н.		

КОНСУЛЬТАНТЫ ПО РАЗДЕЛАМ:

По разделу «Финансовый менеджмент, ресурсоэффективность и ресурсосбережение»

Должность	ФИО	Ученая степень, звание	Подпись	Дата
Доцент ОСГН ШИП	Спицына Л.Ю.	к.ф.н.		

По разделу «Социальная ответственность»

Должность	ФИО	Ученая степень, звание	Подпись	Дата
Доцент ОЯТЦ ИЯТШ	Веригин Д.А.	к.ф-м.н		

ДОПУСТИТЬ К ЗАЩИТЕ:

Руководитель ООП	ФИО	Ученая степень, звание	Подпись	Дата
Nuclear medicine / Ядерная медицина	Верхотурова В.В.	к.и.н.		

Томск – 2021 г.

TOMSK POLYTECHNIC UNIVERSITY
ТОМСКИЙ ПОЛИТЕХНИЧЕСКИЙ УНИВЕРСИТЕТ

Министерство науки и высшего образования Российской Федерации
федеральное государственное автономное
образовательное учреждение высшего образования
«Национальный исследовательский Томский политехнический университет» (ТПУ)

School of Nuclear Science & Engineering
Field of training (specialty): 14.04.02 Nuclear Science and Technology
Specialization: Nuclear medicine
Nuclear Fuel Cycle Division

MASTER THESIS

Topic of research work
Optical diagnostic of advanced electron accelerators

UDC - 621.384.6:681.784.8

Student

Group	Full name	Signature	Date
0AM9M	Gusvitskii Todor		

Scientific supervisor

Position	Full name	Academic degree, academic rank	Signature	Date
Professor	Alexander P. Potylitsyn	D.Sc. of Physics Sciences		

ADVISERS:

Section “Financial Management, Resource Efficiency and Resource Saving”

Position	Full name	Academic degree, academic rank	Signature	Date
Associate Professor	Luibov Y. Spicyna	PhD		

Section “Social Responsibility”

Position	Full name	Academic degree, academic rank	Signature	Date
Associate Professor	Dan A. Verigin	PhD		

ADMITTED TO DEFENSE:

Programme Director	Full name	Academic degree, academic rank	Signature	Date
Nuclear medicine	Vera V. Verkhoturova	PhD		

Tomsk – 2021

LEARNING OUTCOMES

Competence code	Competence name
Universal competences	
UC(U)-1	Ability to make critical analysis of problem-based situations using the systems analysis approach, and generate decisions and action plans.
UC(U)-2	Ability to run a project at all life-cycle stages.
UC(U)-3	Ability to organize and lead the teamwork and generate a team strategy to achieve the target goal.
UC(U)-4	Ability to use modern communication technologies to realize academic and professional interaction.
UC(U)-5	Ability to analyze and account for cultural diversity in the process of intercultural interaction.
UC(U)-6	Ability to set and pursue individual and professional activity priorities and ways to modify professional activity based on the self-esteem.
General professional competences	
GPC(U)-1	Ability to formulate goals and objectives of the research study, select assessment criteria, identify priorities for solving problems.
GPC(U)-2	Ability to apply modern research methods, evaluate and present the results of the performed research.
GPC(U)-3	Ability to present research outcomes in the form of articles, reports, scientific reports and presentations using computer layout systems and office software packages.
Professional competences	
PC(U)-1	Ability to maintain medical and technical documentation related to medico-physical aspects of radiation therapy, interventional radiology and radionuclide diagnostics and therapy.
PC(U)-2	Ability to ensure radiation safety of personnel, public, and the environment, to carry out monitoring of radiation exposure levels of patients, personnel, public, and the environment.
PC(U)-3	Ability to operate and maintain equipment and tools applied for the medical use of radiation.
PC(U)-4	Ability to manage the quality of physical and technical aspects within radiation therapy, diagnostics, interventional radiology and radionuclide diagnostics and therapy departments in accordance with the specific equipment requirements, regulatory requirements and staffing of a medical organization.
PC(U)-5	Ability to conduct and organize dosimetry planning, clinical dosimetry, quality assurance procedures for radiotherapy, interventional radiology, and radionuclide diagnostics and therapy.
PC(U)-6	Ability to apply knowledge of natural sciences, fundamental laws in the field of nuclear physics and technology, clinical and radiation standards, hygienic measures in nuclear medicine, which is sufficient to study issues associated with medical physics using modern equipment and information technology relying on the latest Russian and international experience.
PC(U)-7	Ability to develop reference books, tables and software containing data for clinical use in dosimetric planning of radiation therapy, radionuclide diagnostics and therapy.

PC(U)-8	Ability to take part in the design and physical and technical equipment development for radiation therapy, diagnostics, interventional radiology and radionuclide diagnostics and therapy, and radiation safety divisions.
PC(U)-9	Ability to conduct training sessions and develop instructional materials for the training courses within the cycle of professional training programs (bachelor degree programs).

TOMSK POLYTECHNIC UNIVERSITY — ТОМСКИЙ ПОЛИТЕХНИЧЕСКИЙ УНИВЕРСИТЕТ

Министерство науки и высшего образования Российской Федерации
федеральное государственное автономное
образовательное учреждение высшего образования
«Национальный исследовательский Томский политехнический университет» (ТПУ)

School of Nuclear Science & Engineering
Field of training (specialty): 14.04.02 Nuclear Science and Technology
Specialization: Nuclear medicine
Nuclear Fuel Cycle Division

APPROVED BY:
Program Director
_____________ Verkhoturova V.V.
«____» ____________ 2021

ASSIGNMENT
for the Graduation Thesis completion

In the form:

Master Thesis

For a student:

Group	Full name
0AM9M	Gusvitskii Todor

Topic of research work:

Optical diagnostic of advanced electron accelerators	
Approved by the order of the Director of School of Nuclear Science & Engineering (date, number):	№ 104-43/c dated April 14, 2021

Deadline for completion of Master Thesis:	05.06.2021

TERMS OF REFERENCE:

Initial data for research work: *(the name of the object of research or design; performance or load; mode of operation (continuous, periodic, cyclic, etc.); type of raw material or material of the product; requirements for the product, product or process; special requirements to the features of the operation of the object or product in terms of operational safety, environmental impact, energy costs; economic analysis, etc.)*	Optical transition and diffraction radiation, spatial intensity distribution, electron beam, electron bunch, rectangular slit, circular aperture, optical system, simulation, Wolfram Mathematica software package.

List of the issues to be investigated, designed and developed *(analytical review of literary sources with the purpose to study global scientific and technological achievements in the target field, formulation of the research purpose, design, construction, determination of the procedure for research, design, and construction, discussion of the research work results, formulation of additional sections to be developed; conclusions).*	1. Simulation of coherent optical transition radiation (COTR) field asymmetrically collected by a lens on a detector plane. 2. Finding a dependence between transverse size of simulated electron bunch and some specific parameter of COTR intensity distributions. 3. Simulation of optical transition radiation (OTR) PSFs under non-ideal focusing conditions. 4. Simulation of optical transition radiation (OTR) intensity distributions from electron bunch under non-ideal focusing conditions. 5. Defining a dependence between parameters of obtained distributions and the value of positioning error. 6. Simulation of optical diffraction radiation (ODR) field emitted from a rectangular slit and collected by a lens on a detector plane. 7. Finding a dependence that shows how strong initial electron offset affects symmetry of ODR intensity distribution. 8. Creation of an algorithm for simulation of ODR intensity distribution from a target with a circular aperture. 9. Defining a dependence that connects electron position within the aperture with generated intensity patterns.
List of graphic material *(with an exact indication of mandatory drawings)*	Presentation

Advisors to the sections of the Master Thesis
(with indication of sections)

Section	Advisor
Social responsibility	Dan A. Verigin
Financial Management, Resource Efficiency and Resource Saving	Luibov Y. Spicyna

Date of issuance of the assignment for Master Thesis completion according to the schedule	15.03.2021

Assignment issued by a scientific supervisor / advisor (if any):

Position	Full name	Academic degree, academic status	Signature	Date
Professor	Alexander P. Potylitsyn	D.Sc. of Physics Sciences		

Assignment accepted for execution by a student:

Group	Full name	Signature	Date
0AM9M	Gusvitskii Todor		

ASSIGNMENT FOR THE DIPLOMA PROJECT SECTION
«FINANCIAL MANAGEMENT, RESOURCE EFFICIENCY AND RESOURCE SAVING»

Student:

Group	Name
0AM9M	Gusvitskii Todor

School	School of Nuclear Science & Engineering	**Department**	Division for Nuclear-Fuel Cycle
Educational level	Master	**Specialization**	14.04.02 Nuclear Science and Technology

Initial data for the section "Financial Management, Resource Efficiency and Resource Saving":	
1. The cost of scientific research resources: material, technical, energy, financial, informational and human	*Budget of research not higher than 153695 rubles, salaries of executors not higher than 50775 rubles*
2. Norms and standards for spending resources	*Supervisor' salary – 33775 rubles per month; engineer' salary – 17000 rubles per month*
3. The system of taxation used, tax rates, volumes of payments, discounts and loans	*The amount of insurance premiums is 30%* *Reduced rate in Tomsk - 27,1%*
Problems to research, calculate and describe:	
1. Assessment of the commercial potential of engineering solutions	*Competitive technical solutions evaluation map*
2. Planning of research and constructing process and making schedule for all periods of the project	*Hierarchical structure of work*
3. Requirement for investments	*Costs calculations*
4. Budgeting an engineering project	*Creation of the project budget*
5. Calculation of resource, financial, social, budgetary efficiency of an engineering project and potential risks	*Evalution of technical solutions competitiveness* *SWOT Matrix* *Schedule and budget for the scientific research* *Gantt Chart*
Graphic materials	
1. Evaluation of the competitiveness of technical solutions *2. SWOT- analysis* *3. Gantt chart and budget of scientific research* *4. Assessment of resource, financial and economic efficiency of STR* *5. Potential risks*	

Assignment date	

Consultant:

Position	Name	Academic degree	Signature	Date
Associate Professor Division for Social Sciences and Humanities School of Core Engineering Education	Spicyna Luibov Yurievna	PhD		

Student:

Group	Name	Signature	Date
0AM9M	Gusvitskii Todor		

ASSIGNMENT FOR THE DIPLOMA PROJECT SECTION
«SOCIAL RESPONSIBILITY»

To student:

group	Full name
0AM9M	Gusvitskii Todor

School	**Nuclear Science and Engineering**	**Department**	**Nuclear fuel cycle**
Degree	Master programme	**Specialization**	Nuclear Medicine

Title of graduation thesis:

Optical diagnostic of advanced electron accelerators	
Initial data for section «Social Responsibility»:	
1. Information about object of investigation (matter, material, device, algorithm, procedure, workplace) and area of its application	Beams of electron accelerators. Application area: beam diagnostics
List of items to be investigated and to be developed:	
1. Legal and organizational issues to provide safety: – Special (specific for operation of objects of investigation, designed workplace) legal rules of labor legislation; – Organizational activities for layout of workplace.	– Labour code of Russian Federation #197 from 30/12/2001 GOST 12.2.032-78 SSBT – Sanitary Rules 2.2.2/2.4.1340-03. Hygienic requirements for PC and work with it
2. Work Safety: 2.1. Analysis of identified harmful and dangerous factors 2.2. Justification of measures to reduce probability of harmful and dangerous factors	– Enhanced electromagnetic radiation level – Insufficient illumination of workplace – Excessive noise – Deviation of microclimate indicators – Electric shock
3. Ecological safety:	– Indicate impact of linear accelerator on hydrosphere, atmosphere and lithosphere
4. Safety in emergency situations:	– Fire safety;

Assignment date for section according to schedule	

The task was issued by consultant:

Position	Full name	Scientific degree, rank	Signature	date
Associate Professor Division for Nuclear-Fuel Cycle School of Nuclear Science & Engineering	Verigin D.A.	Cand.of Sc.		

The task was accepted by the student:

Group	Full name	Signature	date
0AM9M	Gusvitskii Todor		

TOMSK POLYTECHNIC UNIVERSITY
ТОМСКИЙ ПОЛИТЕХНИЧЕСКИЙ УНИВЕРСИТЕТ

Министерство науки и высшего образования Российской Федерации
федеральное государственное автономное
образовательное учреждение высшего образования
«Национальный исследовательский Томский политехнический университет» (ТПУ)

School of Nuclear Science & Engineering
Field of training (specialty): 14.04.02 Nuclear Science and Technology
Specialization: Nuclear medicine

Level of education: Master degree program
Nuclear Fuel Cycle Division
Period of completion: spring semester 2020/2021 academic year

Form of presenting the work:

Master Thesis

SCHEDULED ASSESSMENT CALENDAR
for the Master Thesis completion

Deadline for completion of Master's Graduation Thesis:	18.06.2021

Assessment date	Title of section (module) / type of work (research)	Maximum score for the section (module)
15.03.2021	*Drawing up the technical assignment*	…
20.03.2021	*Calendar planning*	
30.03.2021	*Literature review*	
15.04.2021	*Development and preparation of simulation algorithms*	
30.04.2021	*Carrying out calculations according to simulation algorithms*	
10.05.2021	*Summarizing results of all previous works*	
15.05.2021	*Preparation of a final report*	
18.06.2021	*Masters's Thesis defense*	

COMPILED BY:
Scientific supervisor:

Position	Full name	Academic degree, academic status	Signature	Date
Professor	Alexander P. Potylitsyn	D.Sc. of Physics Sciences		

APPROVED BY:

Program Director	Full name	Academic degree, academic status	Signature	Date
Nuclear medicine	Vera V. Verkhoturova	PhD		

ABSTRACT

Master's Graduation work 86 p., 31 fig., 20 tab., 15 sources.

Keywords: FLASH, XFEL, electron beam diagnostic, electron bunch size, electron beam position monitor, optical transition radiation, optical diffraction radiation, point spread function, intensity distributions, fitting function, protein vehicle, microCT angiography.

Objects of research are non-invasive diagnostic methods for electron beams used for research purposes in advanced accelerator facilities.

Purpose of the work is to develop non-invasive optical methods that allow determining such electron bunch parameters as transverse size and position.

During the current work the following research processes were conducted: coherent optical transition radiation intensity distributions were simulated under conditions of partial focusing or asymmetrical light collection for the purpose of developing modified method of transverse bunch size measurements; the effect of non-ideal focusing conditions on OTR light collection was also studied through the simulation; the feasibility of optical diffraction radiation beam position monitors based on rectangular and round slit was also analyzed. Every corresponding simulation was carried out in Wolfram Mathematica software package.

The results of conducted research include improvement of the method for determining transverse size of the electron bunch via coherent optical transition radiation and two approaches for electron beam position monitoring solutions based on optical diffraction radiation. Results for non-ideal focusing conditions are also presented.

List of abbreviations

Abbreviations used in the work:

FLASH – Free Electron LASer in Hamburg

FEL – Free Electron Laser

European XFEL – European X-Ray Free-Electron Laser Facility

TR – Transition Radiation

OTR – Optical Transition Radiation

COTR – Coherent Optical Transition Radiation

DR – Diffraction Radiation

ODR – Optical Diffraction Radiation

PSF – point spread function

FWHM – Full Width at Half Maximum

Contents

Introduction

Electron beam diagnostics via transition and diffraction radiation are one of the main and conventional methods of beam diagnostic for linear electron accelerators. Both of these radiation types can be explained by polarization mechanism when a charged particle's field induces polarization of atoms within the medium which has some dielectric permittivity value. The only difference is that the transition radiation is emitted when a particle with some charge crosses the boundary between two media of different dielectric permittivity values and directly interacts with such media. On the contrary, diffraction radiation is only emitted when a charged particle travels near such boundary, i.e. only the Coulomb field of the particle experiences direct interactions with the target media. A schematic representation for both transition and diffraction is shown in Figure 1.

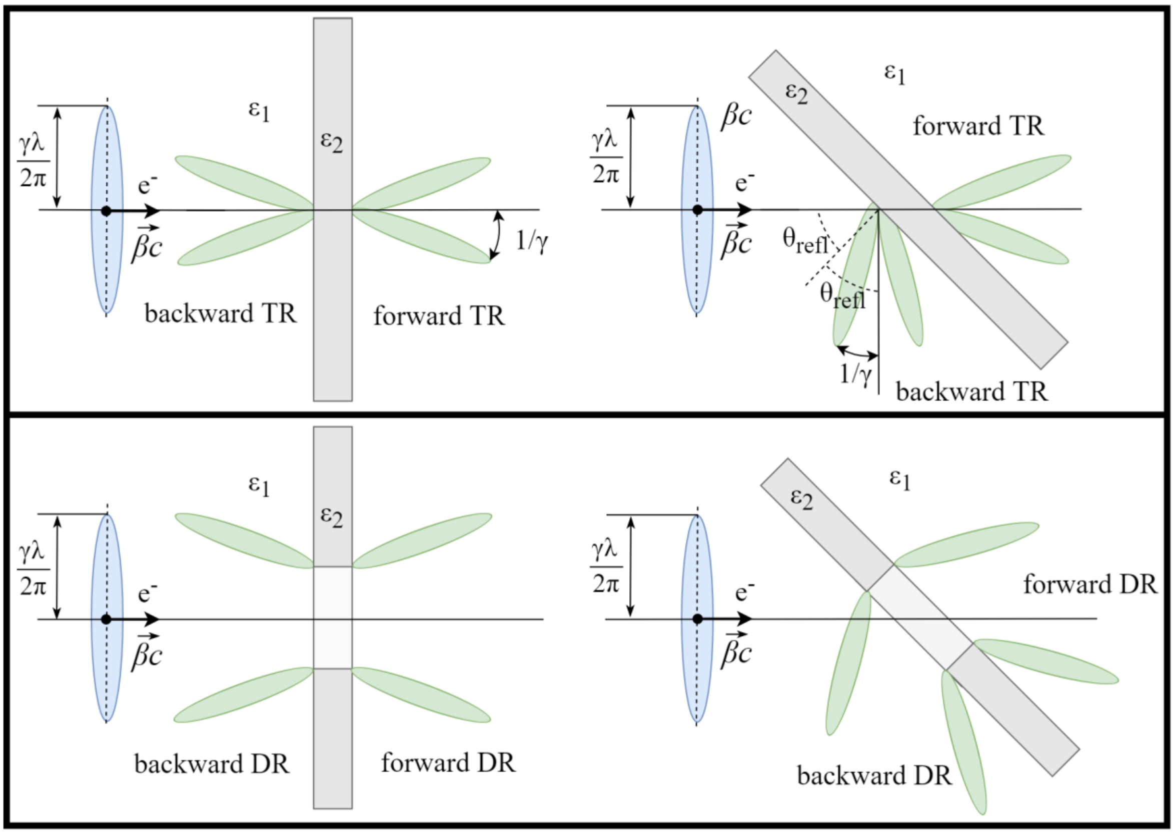

Fig. 1. Scheme describing transition (at the top) and diffraction (at the bottom) radiation generation and its propagation. ε_2 – target permittivity, $\varepsilon_1 = 1$ – vacuum.

The emission of transition and diffraction radiation occurs in two possible directions: forward and backward. The part of radiation that propagates in forward direction always goes along a charged particle's trajectory, regardless of its incident angle. The backward part of radiation is directed along the reflection angle to the surface of the medium. The angular distribution of both parts has cone-like shape with zero intensity along its axis and maxima at the angle of $1/\gamma$ to the central axis of the cone, where γ is the Lorentz factor of the incident particle [1].

The application of backward transition and diffraction radiation for beam diagnostic purposes is basically more attractive due to low background than the application of the forward one. Other advantage is the following - detecting system can be placed relatively far from the beamline.

In recent years, radiopharmaceuticals are widely spread in nuclear medicine for diagnostic and therapeutic purposes. A wide range of radiopharmaceuticals are based on protein vehicles. The efficiency of such delivery platforms is defined by the amount of research works done to understand how these particles behave while interacting with cells in human organism. High-quality research of biological and chemical outcomes of protein carrier systems cannot be carried out in compact laboratories with relatively simple analyzing tools and usually involves large-scale research accelerators such as FLASH and XFEL located in Hamburg, Germany. Those facilities provide photon emission with high monochromaticity factor in ultraviolet and X-ray spectrum correspondingly which allows observation of all chemobiological reactions on subatomic level. The higher the quality of the electron beam producing the photon emission the more precise and complex observations of chemical and biological reactions could be made.

In addition, in modern times, electron accelerators with energies up to 20 MeV are widely used for radiation therapy (Siemens, Elekta and etc.). In recent years, new accelerating machines have been developed that provide monochromatic x-ray beams which, in turn, could be used not only for treatment, but also for angiography of blood vessels [2,3]. X-ray beams that are fit for this purpose should possess monochromaticity factor of about 1% and transverse size less than 1 mm, and requirements for such beams' parameters are correspondingly high.

Therefore, the current work is focused on the different methods of electron beam diagnostic via OTR and ODR including proposals for beam position monitoring and transverse bunch size measurements with less than 10 μm resolution.

1 OTR for diagnostic purposes of electron beams

1.1 Transverse bunch size measurements via COTR

In XXI century, exploitation of the laser-based acceleration technologies made it possible to obtain and accelerate electron bunches with femtosecond duration [2,3]. Transition radiation from these bunches becomes coherent in the optical bandwidth, and, therefore, conventional methods of beam diagnostic based on focusing of incoming radiation lose their applicability.

Image obtained on the detector possesses ring structure, which, in contrast to the single maximum pattern, has no corresponding algorithm for transverse beam size reconstruction yet [4]. Model, which connects transverse beam size with the radius of the ring structure, is presented in the work [5]. The method of improving spatial resolution for conventional optic system suggested in the current work is based on the work [6].

1.1.1 Theory

Spectral-angular distribution of coherent transition radiation can be described by the next formula [7]:

$$\frac{d^2W}{d\omega d\Omega} = N\frac{d^2W^{inc}}{d\omega d\Omega} + N(N-1)\frac{d^2W^{coh}}{d\omega d\Omega}. \quad (1)$$

Where $\frac{d^2W^{inc}}{d\omega d\Omega}$ – incoherent component of the transition radiation; $\frac{d^2W^{coh}}{d\omega d\Omega}$ – coherent component of the transition radiation; N – number of particles in the bunch.

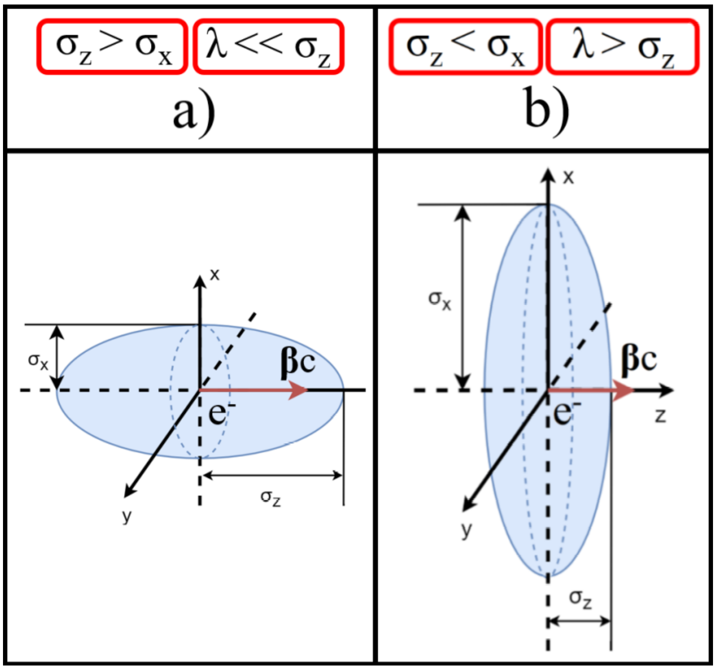

Fig. 2. Electron bunch shapes for incoherent case (a) and coherent case (b)

On most conventional linear accelerators electron beam's bunches have the shape of an ellipsoid that stretches along the beam trajectory, whose longitudinal size is much bigger than transverse one (Figure 2a). Intensity distribution for such bunches will have only one maximum. For the case when $\sigma_z >> \lambda$ first part of the expression (1) corresponding to incoherent radiation will exceed the second one in several times.

Laser-driven plasma wakefield accelerators allow to generate electron bunches of femtosecond duration and they've got shape of an ellipsoid whose longitudinal size is less than the transverse one $\sigma_z < \sigma_x$ (Figure. 2b). Transition radiation from bunches like that has predominant coherent component if condition $\sigma_z \lesssim \lambda$ is not violated, which allows one to omit the firs term of the expression (1).

1.1.2 Model for simulation

Simulation of the results which are presented here were carried out in Wolfram Mathematica. For the sake of simplification and visibility all distributions and fields are presented as one dimensional functions for only one polarization component of OTR (horizontal one, see Figure 3).

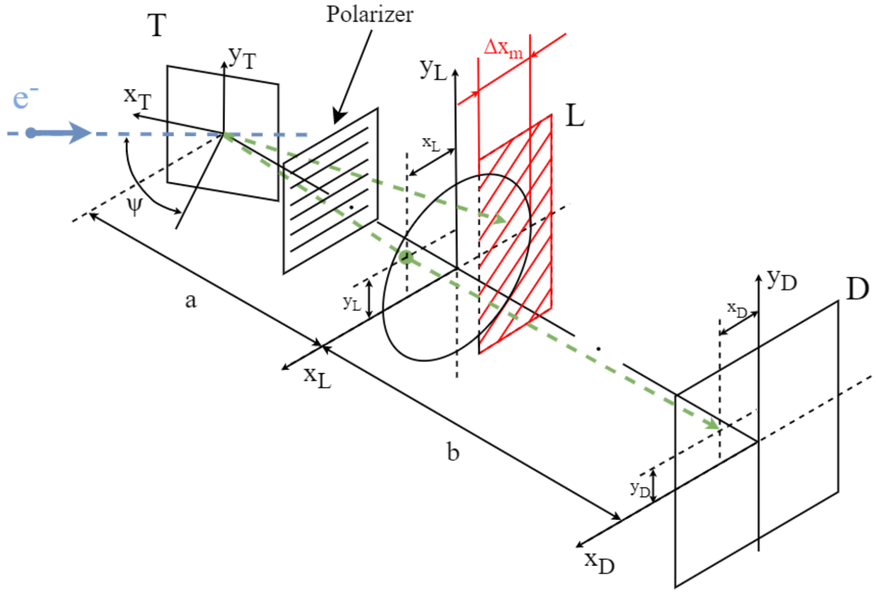

Fig. 3. Scheme of optical system for coherent optical transition radiation focusing consisting of a target (T), a lens (L) and detector (D). *Ψ* – electron incident angle.

Calculation for OTR field x-component was carried out by the following formula [5]:

$$E^{D}_{\{x,y\}}\left(x_D,y_D,x_0,y_0\right)=const\int dx_T dy_T dx_L dy_L \frac{\{x_T-x_0,y_T-y_0\}}{\sqrt{\left(x_T-x_0\right)^2+\left(y_T-y_0\right)^2}}\times$$
$$\times K_1\left(\sqrt{\left(x_T-x_0\right)^2+\left(y_T-y_0\right)^2}\right)\exp\left[i\frac{x_T^2+y_T^2}{4\pi R}\right]\times \quad (2)$$
$$\times\exp\left[-i\left(x_T x_L+y_T y_L\right)\right]\exp\left[-i\left(x_L\frac{x_D}{M}+y_L\frac{y_D}{M}\right)\right].$$

Following units were used in expression (2): $\{x_T,y_T\}=\frac{2\pi}{\gamma\lambda}\cdot\{X_T,Y_T\}$ – coordinates on the target plane; $\{x_L,y_L\}=\frac{\gamma}{a}\cdot\{X_L,Y_L\}$ – coordinates on the lens plane; $\{x_D,y_D\}=\frac{2\pi}{\gamma\lambda}\cdot\{X_D,Y_D\}$ – coordinates on the detector plane in dimensionless units; $R=\frac{a}{\lambda\gamma^2}$ – parameter that describes far field wave zone [8]; $x_0=\frac{2\pi}{\gamma\lambda}*X_0$ – incident electron's shift from the center of the target along its x axis; *M* is the lens optical amplification, K_1 is the modified Bessel function.

Integration of the expression (2) is carried out over the target surface and lens aperture.

It was shown in work [9] that focusing of full cone of COTR by conventional optical system results in a ring structured intensity distribution on the detector.

Method of asymmetrical OTR collection by covering the half of the lens aperture by opaque mask (in other words, blocking one half of OTR cone; OTR was polarized perpendicularly to the mask's edge) was discussed in the paper [6]. Such manipulations with the lens of an optical system leads to significant changes in intensity distribution's shape: it loses its ring structure and acquires only one maximum located in the center of the image. That method allows to increase the resolution of measurements in comparison to the conventional one.

To obtain the expression for the OTR field in case of half-covered lens the integrand that corresponds to lens aperture in the expression (2) should be calculated analytically over the following regions $-x_m + \Delta x_m \le x_L \le x_m, -y_m \le y_L \le y_m$:

$$\int_{-x_m+\Delta x_m}^{x_m} dx_L \int_{-y_m}^{y_m} dy_L \exp\left[-i\left(x_T x_L + y_T y_L\right)\right] \exp\left[-i\left(x_L \frac{x_D}{M} + y_L \frac{y_D}{M}\right)\right] = \\ = \frac{2i\left(e^{i\frac{x_m}{M}\left(x_D + M\cdot x_T\right)} - e^{\frac{i}{M}\left(x_D + M\cdot x_T\right)\left(x_m + \Delta x_m\right)}\right) M^2 \sin\left[y_m\left(\frac{y_D}{M} + y_T\right)\right]}{\left(x_D + M\cdot x_T\right)\left(y_D + M\cdot y_T\right)}. \qquad (3)$$

For simplification, the lens in the expression (3) was considered as square. Δx_m defines the covered part of the lens.

Substituting (3) in the expression for x-component of the OTR field (2) one gets the following formula:

$$E_x^D\left(x_D, y_D, x_0, y_0\right) = const \int dx_T dy_T \frac{x_T - x_0}{\sqrt{\left(x_T - x_0\right)^2 + \left(y_T - y_0\right)^2}} \times \\ \times K_1\left(\sqrt{\left(x_T - x_0\right)^2 + \left(y_T - y_0\right)^2}\right) \exp\left[i\frac{x_T^2 + y_T^2}{4\pi R}\right] \times \\ \times \frac{2i\left(e^{i\frac{x_m}{M}\left(x_D + M\cdot x_T\right)} - e^{\frac{i}{M}\left(x_D + M\cdot x_T\right)\left(x_m + \Delta x_m\right)}\right) M^2 \sin\left[y_m\left(\frac{y_D}{M} + y_T\right)\right]}{\left(x_D + M\cdot x_T\right)\left(y_D + M\cdot y_T\right)}. \qquad (4)$$

Intensity for x-component of the OTR can be calculated by conventional formula:

$$\frac{d^2W_x^D}{dx_D dy_D}(x_D, y_D, x_0, y_0) = const\left|E_x^D(x_D, y_D, x_0, y_0)\right|^2. \tag{5}$$

1.1.3 Simulation results

Figure 4 represents some calculation results of the OTR intensity distribution in case of single electron incidence (so-called “point spread function”, PSF) for different degrees of lens screening.

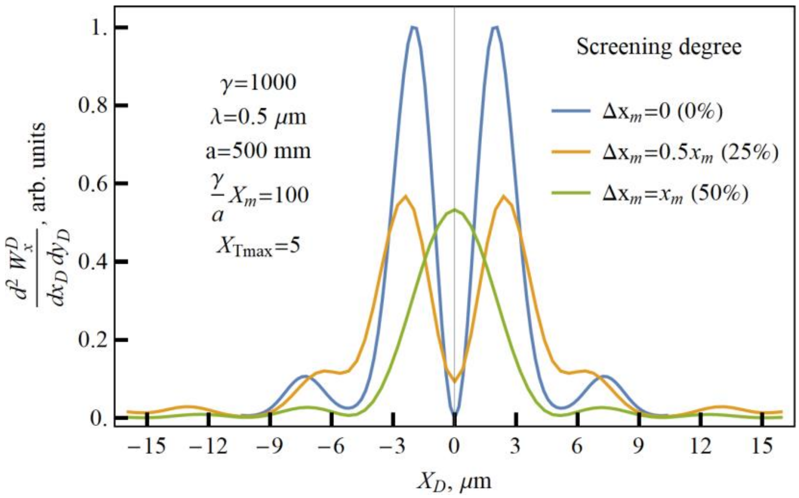

Fig. 4. PSF for various screening degrees

As can be seen from the result above, with the increase of the screening rate values the shape of distribution changes from two-lobe form to the form which possesses only one maximum for the case of half-covered lens. This result can be explained in the following way: screen that covers half of the lens also blocks one half of OTR cone which, basically, means that only one maximum will be visible on the image.

In case of incoherent optical transition radiation these PSFs can be used to directly obtain the image of the bunch by convolution with charge distribution within the bunch. However, in case of coherent optical transition radiation so-called FPSF [9] must be used (field point spread function), because, in that case, summation goes over each electron’s field in the bunch.

FPSFs can be calculated by expressions (2) and (4) for the case of non-covered and half-masked lens correspondingly. Figure 5a contains results of FPSF's real part calculation for both cases mentioned above.

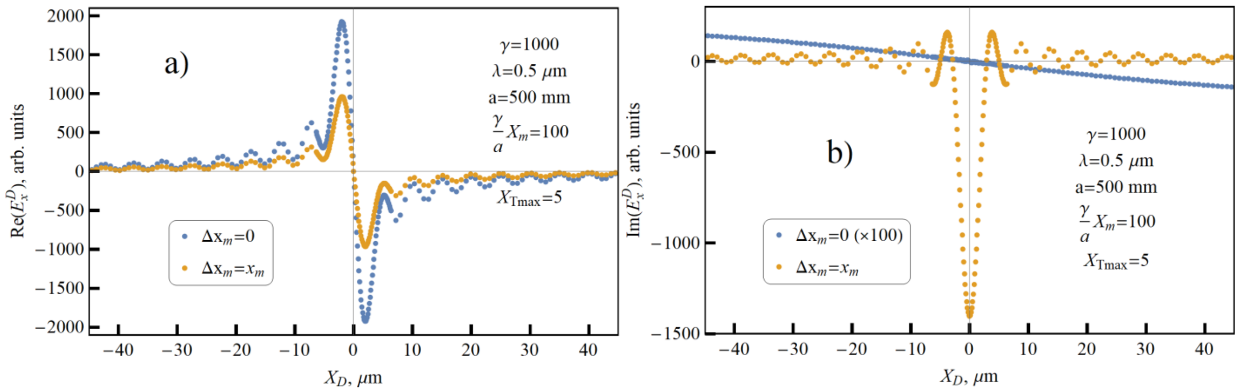

Fig 5. Real (a) and imaginary (b) parts of the OTR field in case of non-covered and half-masked lens

Figure 5b shows the imaginary part of the OTR field for both cases. The one that corresponds to open lens is magnified hundred times to be more visible. Therefore, it can be concluded that imaginary part for open lens case can be omitted due to its insignificant values. On the contrary, imaginary part of the OTR field for the case of half-covered lens becomes quite significant, not to mention the fact that its maximum amplitude is even higher than the corresponding amplitude of the real part and that is exactly what contributes the most to the one-lobbed shape of the intensity distribution.

Considering the fact that all electrons in the bunch with the size of our field of interest emit coherently resulting field of COTR from the bunch can be obtained by a convolution of OTR field from a single electron with the function $\rho(x_0, y_0)$. The following approach will be used:

$$\rho\left(x_0, y_0\right) = \frac{1}{2\pi\sigma_x\sigma_y}\exp\left[-\frac{x_0^2}{2\sigma_x^2} - \frac{y_0^2}{2\sigma_y^2}\right], \qquad (6)$$

where $\sigma_{\{x,y\}} = \frac{2\pi}{\gamma\lambda} * \Sigma_{\{x,y\}}$ is a bunch size along x and y axis in dimensionless units.

As it was shown in the paper [5], shape of FPSF can be considered constant among all electrons in the bunch with the sizes that correspond to the field of interest of this paper. That fact significantly simplifies the process of calculations and, instead of using expressions (2) and (4), one can exploit relatively simple approximation functions.

For the real part of the FPSF either in case of open lens or in case of the half-masked one the following odd function can be chosen for approximation:

$$\mathrm{Re}\left(E_x^D\left(x_D\right)\right)=a_0 x_D \exp\left[-b_0 x_D^2\right]+\sum_{k=1}^{i} a_k \sin\left[b_k x_D\right]=FPSF_x\left(x_D\right). \tag{7}$$

Number of summands was chosen equal to i = 25. Full information about parameters' value of this fitting function can be found in the work [5]. Results of the approximation are shown in Figure 6a.

In turn, the imaginary part of the FPSF for the case of half-masked lens can be fitted by the following even function:

$$\mathrm{Im}\left(E_x^D\left(x_D\right)\right)=\frac{a_0}{2}+\sum_{k=1}^{i}\cos[k\cdot x_D]a_k. \tag{8}$$

Number of summands is set to i = 90.

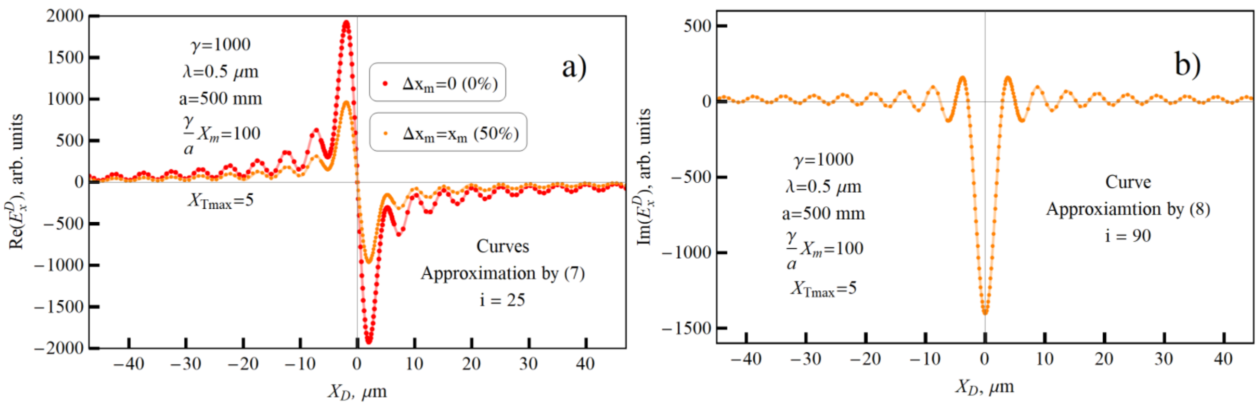

Fig. 6. Real (a) and imaginary (b) parts of FPSF and corresponding fitting functions for the open lens and the masked one.

Approximation functions obtained can be convoluted with the expression (6) in one-dimensional form (for simplification) to get the total OTR field from all electrons in the bunch cross-section:

$$E_{coh\ x}^D\left(x_D,\sigma_x\right)=const\int_{-3.5\sigma_x}^{3.5\sigma_x} dx_0\rho\left(x_0\right)FPSF_x\left(x_D-x_0\right). \tag{9}$$

Hence, the intensity distribution of COTR in the plane of a detector can be found through the following formula:

$$\frac{d^2W_x^{coh}}{dx_D dy_D}(x_D,\sigma_x) = const\left|E^D_{coh\ x}(x_D,\sigma_x)\right|^2. \qquad (10)$$

Corresponding results are depicted in Figure 8.

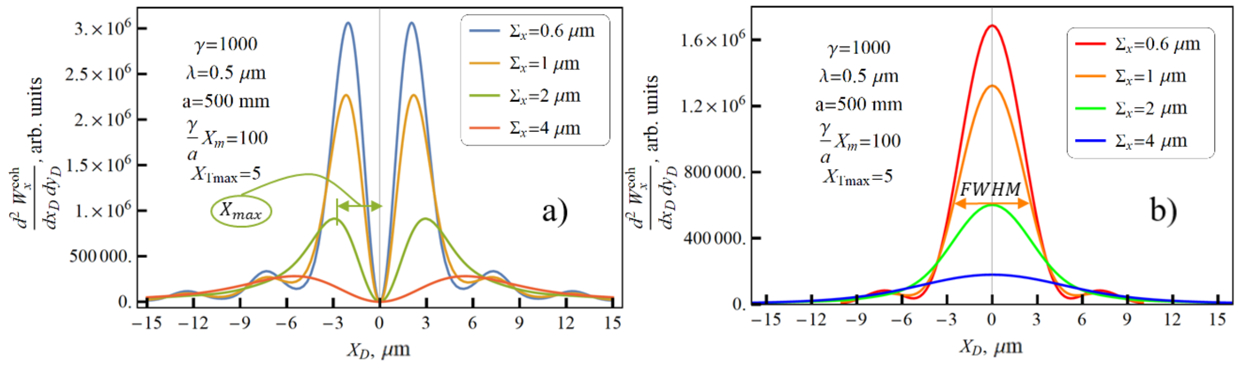

Fig. 7. COTR intensity distributions from electron bunches of micron transverse sizes. a) lens without screening; b) masked lens

Like the PSF, COTR intensity distribution also alters its shape from two-lobe structure to the distribution with only one central maximum when mask is applied. The full width at half maximum (FWHM) for the latter case can be used to define the dependence between this parameter and transverse beam size (see Figure 8).

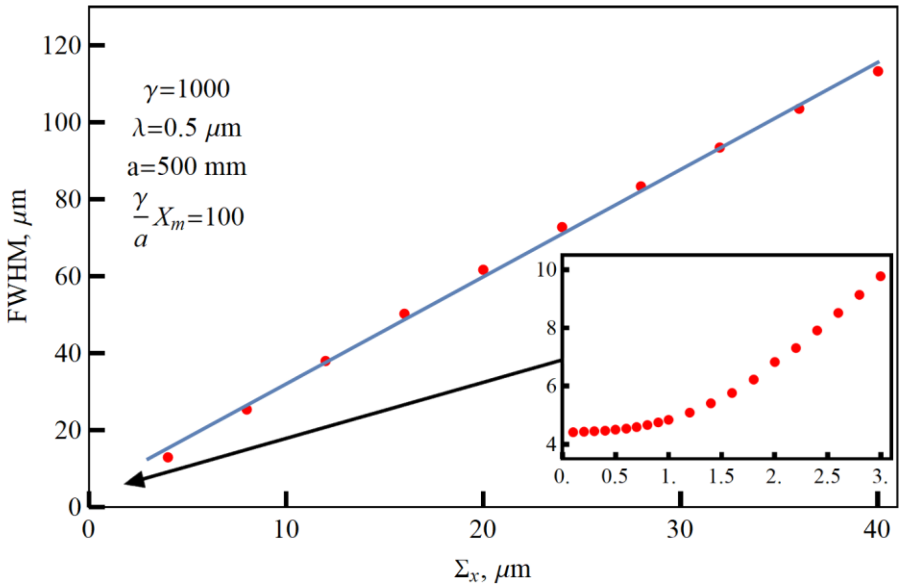

Fig. 8. Dependence between FWHM of the approximation function used and the simulated transverse size (> 3 μm) of the electron bunch (behavior of this dependence in the size region less than 3 μm is shown separately)

This dependence can be easily approximated by the following linear function:

$$FWHM = 4.19\ \mu\text{m} + 2.79\Sigma_x. \qquad (11)$$

The same dependences but for different beam and lens aperture parameters are shown in Figure 9.

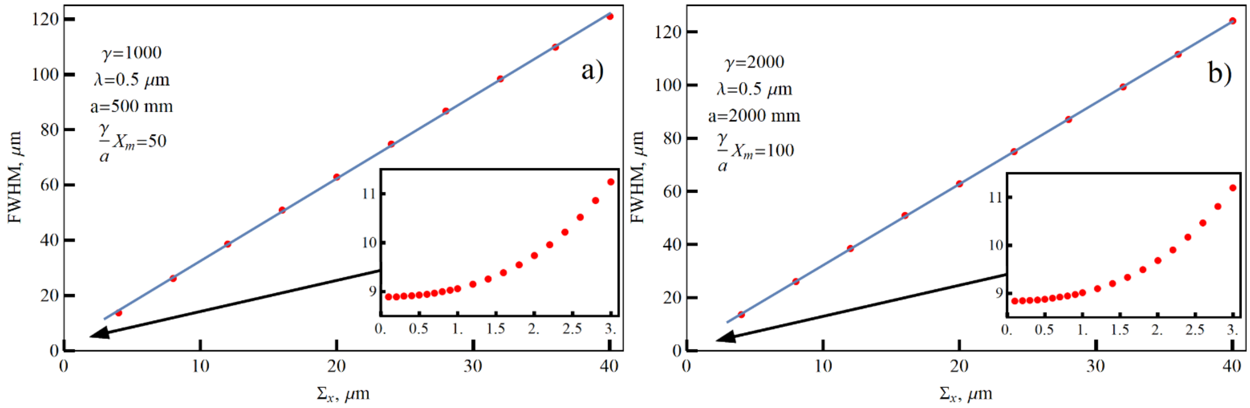

Fig. 9. Dependence between FWHM of the approximation function used and the simulated transverse size of the electron beam for different set of experiment parameters ($\gamma = 1000$, $\frac{\gamma}{a} \cdot X_m = 50$ and $\gamma = 2000$, $\frac{\gamma}{a} \cdot X_m = 100$)

The dependence from the Figure 9a can be described by the following linear expression:

$$FWHM = 2.67\ \mu\text{m} + 2.99\Sigma_x. \qquad (12)$$

The same can be done for the other one from Fig. 9b:

$$FWHM = 1.67\ \mu\text{m} + 3.06\Sigma_x. \qquad (13)$$

1.1.4 Chapter conclusion

This work suggests a method for evaluation of subpicosecond/subfemtosecond electron beam image parameters via COTR focusing. It is shown that covering the half of the lens with opaque screen results in one-lobed structure of the beam image, whereas the lens with no screen produces the beam image with the ring structure.

For electron bunches with the size $\Sigma_x > 3$ μm the dependence between FWHM and unknown parameter Σ_x is linear, which allows one to define the transverse bunch size (FWHM ≈ $3\Sigma_x$, if $\Sigma_x \gg 3$ μm).

For smaller electron bunch transverse sizes ($\Sigma_x \lesssim 3$ μm) mentioned linear dependence is violated and, for that case, some additional analysis should be carried out, e.g. taking measures of FWHM for different values of radiation wavelength.

1.2 Focusing of OTR under non-ideal conditions

1.2.1 Description of the method

The simulation of OTR that is carried out in this chapter is based on optical system scheme presented in Figure 10.

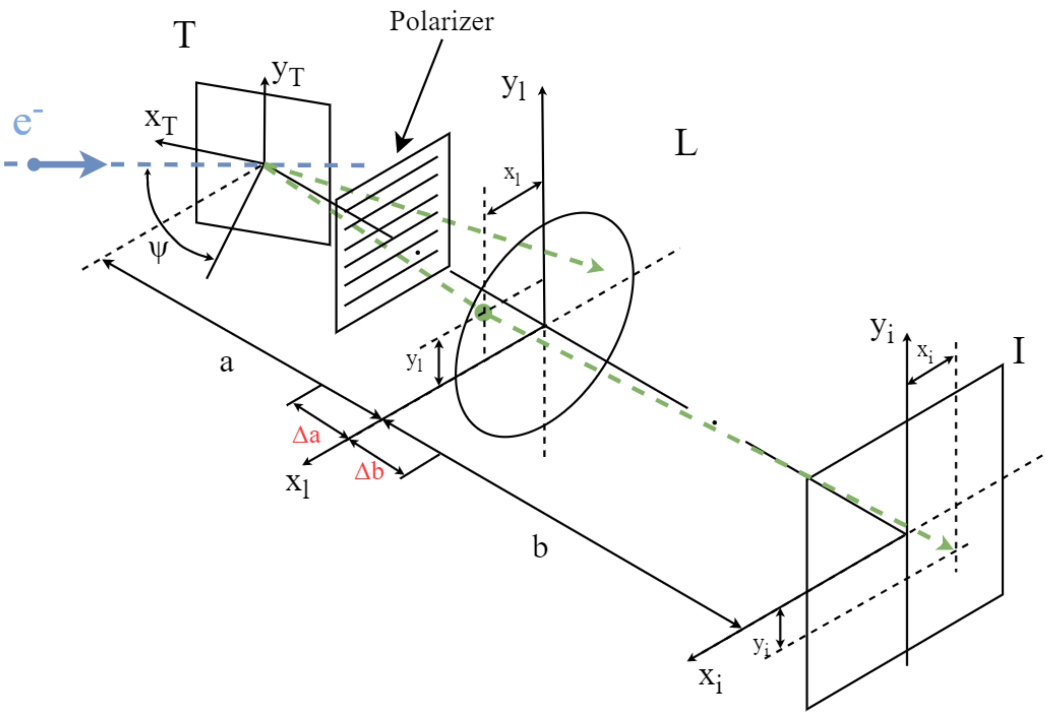

Fig. 10. Scheme of optical system for the case of non-ideal focusing of OTR consisting of a target (T), a lens (L) and image plane (I); Ψ – electron incident angle

OTR field of a single electron, focused at the point $\{x_i, y_i\}$ on the detector plane, in case of ideal lens positioning can be described by the following expression [1]:

$$E^{i}_{x_i,y_i}(x_i, y_i, \lambda) = \frac{2e}{\lambda M \beta c} \frac{\{x_i, y_i\}}{\sqrt{x_i^2 + y_i^2}} \times \int_0^{\theta_m} d\theta \frac{\theta^2}{\theta^2 + (\beta\gamma)^{-2}} \times$$
$$\times J_1\left(\frac{2\pi\sqrt{x_i^2 + y_i^2}\,\theta}{\lambda M}\right) \exp\left(-i\frac{\pi}{\lambda} a^2 \theta^2 \left(\frac{1}{f} - \frac{1}{a} - \frac{1}{b}\right)\right). \quad (14)$$

Here λ is the wavelength of OTR, e is electron charge, $M = \frac{b}{a}$ is the lens optical amplification (magnification), $\beta = \frac{v}{c}$ is electron speed in the units of speed of light, $\theta = \frac{\sqrt{x_l^2 + y_l^2}}{a}$ is a polar angle, $\{x_l, y_l\}$ - lens plane coordinates, $\theta_m = \frac{\sqrt{x_m^2 + y_m^2}}{a}$

- angle aperture of the lens, a is the distance between target and lens, b is the distance between lens and detector. When the lens positioning is ideal (i.e. $\frac{1}{f}=\frac{1}{a}+\frac{1}{b}$) last exponential factor is equal to 1. However, if one considers some shifts in lens positioning, the mentioned factor in expression (14) changes:

$$E^{i}_{x_i,y_i}(x_i,y_i,\lambda)=\frac{2e}{\lambda M^{*}\beta c}\frac{\{x_i,y_i\}}{\sqrt{x_i^2+y_i^2}}\times\int_0^{\theta_m^*}d\theta^{*}\frac{\theta^{*2}}{\theta^{*2}+\left(\beta\gamma\right)^{-2}}\times$$
$$\times J_1\left(\frac{2\pi\sqrt{x_i^2+y_i^2}\theta^{*}}{\lambda M^{*}}\right)\exp\left(-i\frac{\pi}{\lambda}\left(a+\Delta a\right)^2\theta^{*2}\left(\frac{1}{f}-\frac{1}{a+\Delta a}-\frac{1}{b+\Delta b}\right)\right). \tag{15}$$

Where $M^{*}=\frac{b+\Delta b}{a+\Delta a}$ is a coefficient that represents lens magnification power with consideration of some shifts in the position of the lens, $\theta^{*}=\frac{\sqrt{x_l^2+y_l^2}}{a+\Delta a}$ is a polar angle with consideration of shifts in lens position, $\theta_m^{*}=\frac{\sqrt{x_m^2+y_m^2}}{a+\Delta a}$ is an expression for the lens angle aperture that takes into account the shifts along the optical axis, $\Delta a,\Delta b$ are the same mentioned shifts for distances a and b respectively.

To simplify the following calculations and considering field of interest of the work [10], only vertical component of OTR field is observed. Omitting constant values in the expression (15) one gets:

$$E^{i}_{y_i}(x_i,y_i,\lambda)=const\frac{y_i}{M^{*}\sqrt{x_i^2+y_i^2}}\times\int_0^{\theta_m^*}d\theta^{*}\frac{\theta^{*2}}{\theta^{*2}+\left(\beta\gamma\right)^{-2}}\times$$
$$\times J_1\left(\frac{2\pi\sqrt{x_i^2+y_i^2}\theta^{*}}{\lambda M^{*}}\right)\exp\left(-i\frac{\pi}{\lambda}\left(a+\Delta a\right)^2\theta^{*2}\left(\frac{1}{f}-\frac{1}{a+\Delta a}-\frac{1}{b+\Delta b}\right)\right). \tag{16}$$

Therefore, intensity distribution of OTR from a single electron or point spread function (PSF) can be written as follows:

$$\frac{d^2W}{d\omega d\Omega}=const\left|E^{i}_{y_i}\left(x_i,y_i,\lambda\right)\right|^2. \tag{17}$$

To simulate OTR intensity distribution from a whole bunch one should convolute expression for PSF (17) with spatial charge distribution of the bunch (only vertical projection of this distribution in our case):

$$\rho_y\left(y_0,\sigma_y\right)=\frac{1}{\sigma_y\sqrt{2\pi}}\exp\left[-\frac{{y_0}^2}{2{\sigma_y}^2}\right], \tag{18}$$

and, as a result of convolution:

$$\frac{d^2W^{tot}}{d\omega d\Omega}=const\int_{-3,5\sigma_y}^{3,5\sigma_y}\rho_y\left(y_0,\sigma_y\right)\left|E_{y_i}^{i}\left(x_i,y_i-y_0,\lambda\right)\right|^2 dy_0, \tag{19}$$

where σ_y is a transverse size of the electron bunch in a vertical projection, y_0 is the electron position within the bunch according to its center.

1.2.2 Simulation results

Simulation itself was carried out by using Wolfram Mathematica. To give description for observed widening in the work [10], it was decided to use the same beam and set-up parameters for the following simulation.

Using expression (17) it is possible to show how different values of positioning error affect PSF (see Figure 11 and Figure 12).

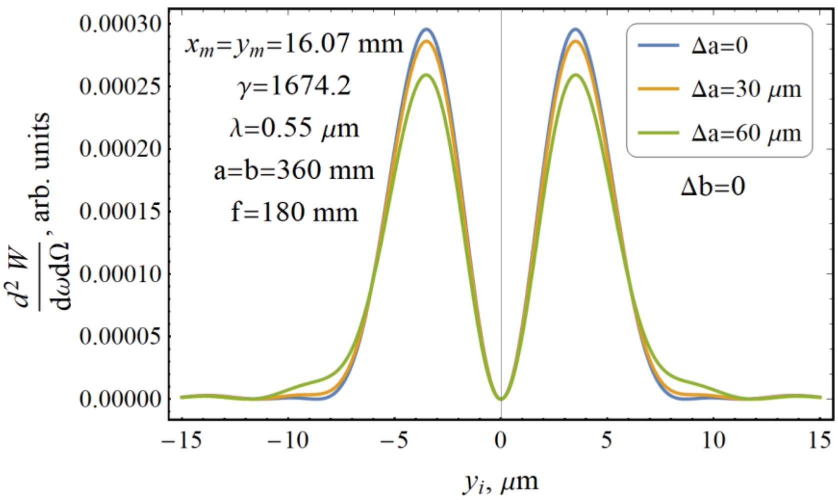

Fig. 11. The change in PSF shape for different positioning errors of micron order

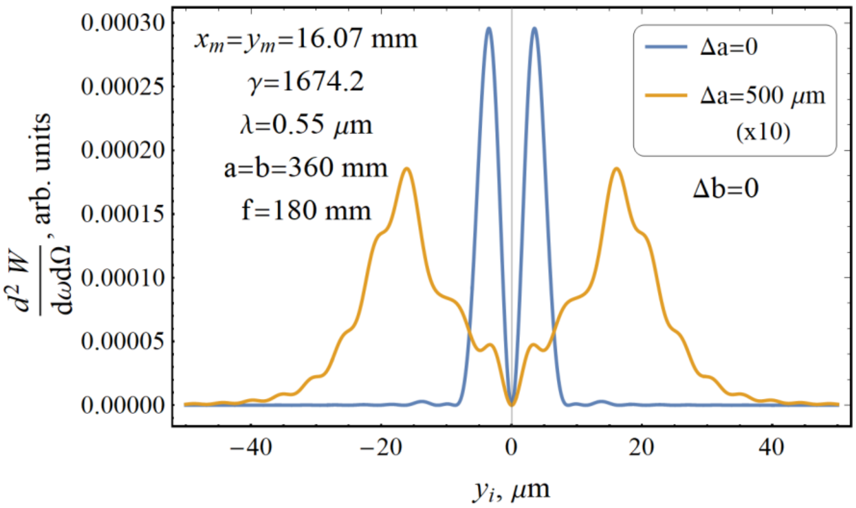

Fig. 12. The change in PSF shape for positioning error of half of millimeter

As can be seen from the Figure 12, the shape of PSF changes dramatically due to significant values of positioning error, additional peak values appear and it becomes practically impossible to define the location of distribution's maximum. So, it also means that the dependence between maximum's position and the positioning error value cannot be defined either. Though it will be shown later that this problem can be partly solved by applying of fitting function to all of the distributions where peak value cannot be clearly found.

The change in the shape of PSF for significant defocusing values (positioning error values) can actually be almost zero if the displacement values *a* and *b* have equal absolute values but the signs are opposite (see Figure 13). But this effect is true only when $|\Delta a|,|\Delta b| \lesssim 2000$ μm because, otherwise, the lens magnification *M* ceases to be equal to 1.

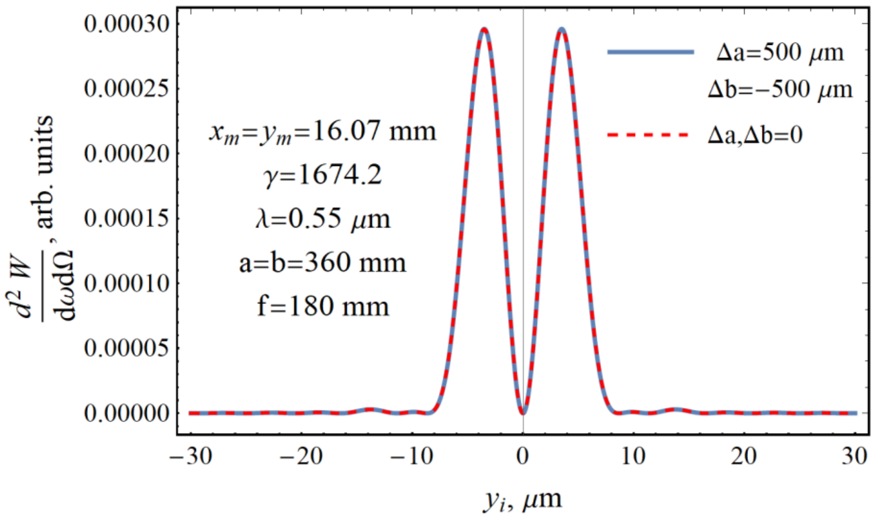

Fig. 13. The change in the shape of PSF is almost zero while $\Delta a + \Delta b = 0$

Convolution of PSFs with spatial charge distribution within electron bunch according to the expression (19) gives the following results (see Figure 14 and Figure 15). The value of Δa is fixed (500 µm).

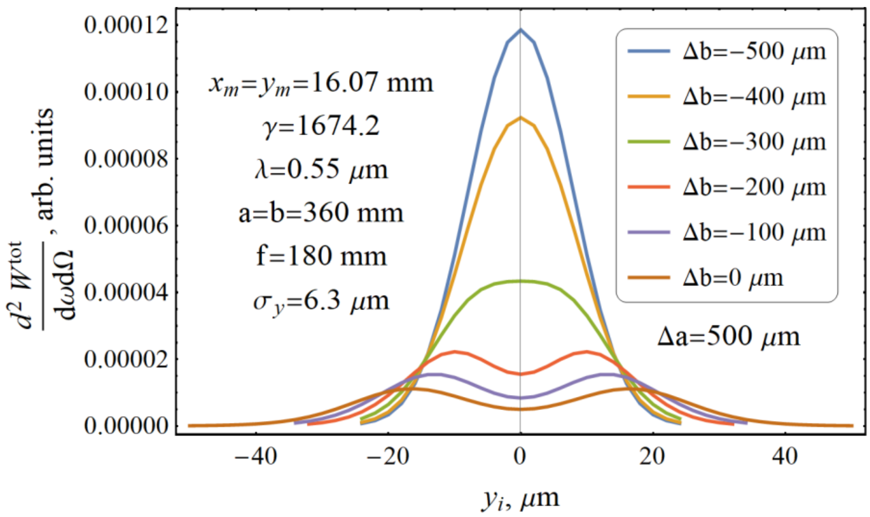

Fig. 14. OTR intensity distributions from electron bunch for different lens displacement values

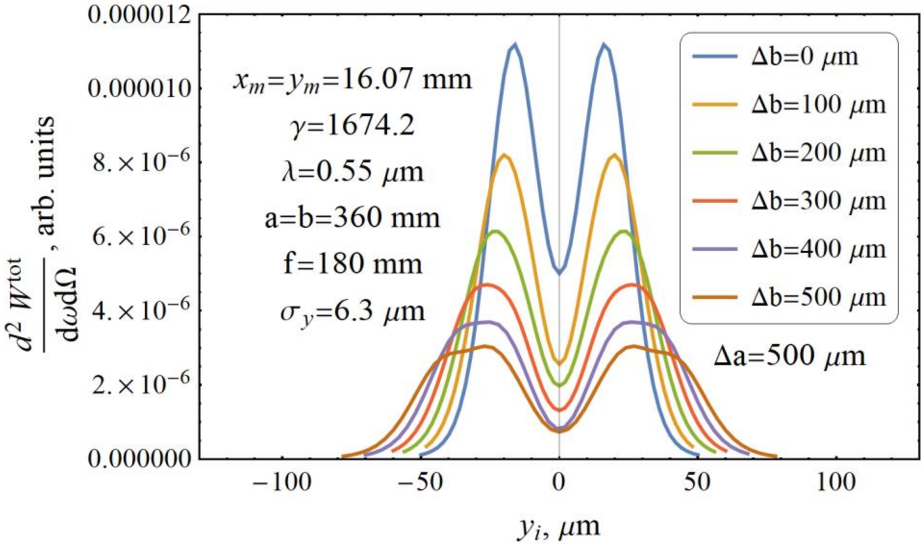

Fig. 15. OTR intensity distributions from electron bunch for different lens displacement values

One can notice that distributions lose Gaussian shape and become double-lobbed if error values exceed $\Delta b = -300$ µm. It basically means that it is possible to find the dependence of FWHM on defocusing grade only for the region of values $\Delta b = -500 ... -300$ µm (if $\Delta a = 500$ µm).

To assess distributions' FWHM these distributions should be fitted by Gaussian function:

$$f\left(y_i\right) = A\exp\left[-\frac{y_i^{\ 2}}{2B^2}\right], \tag{20}$$

where *A*, *B* are parameters of the fitting function which are defined automatically.

An example of such fitted distribution is shown in Figure 16 below.

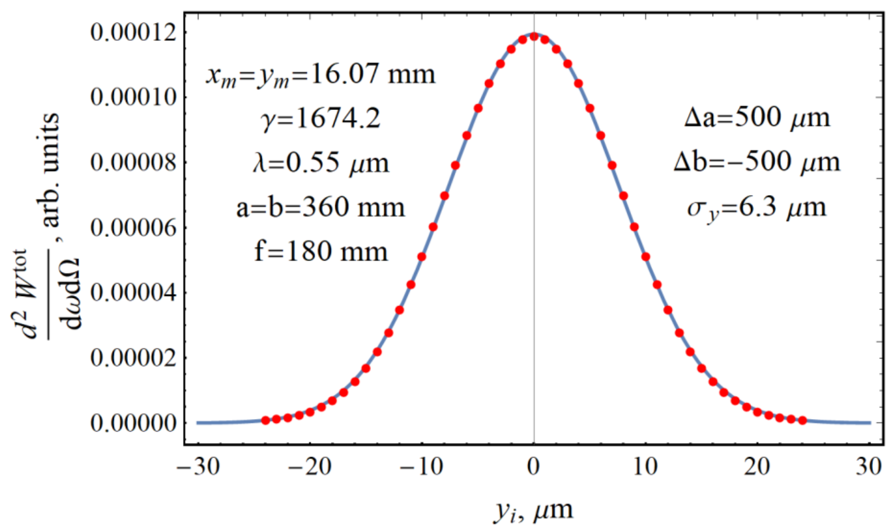

Fig. 16. An example of OTR intensity distribution from the whole bunch being fitted by Gaussian function (20) under non-ideal focusing conditions

FWHM parameter of these fitting functions can be used to plot the dependence between it and the values of positioning error. The dependence itself is presented in Figure 17.

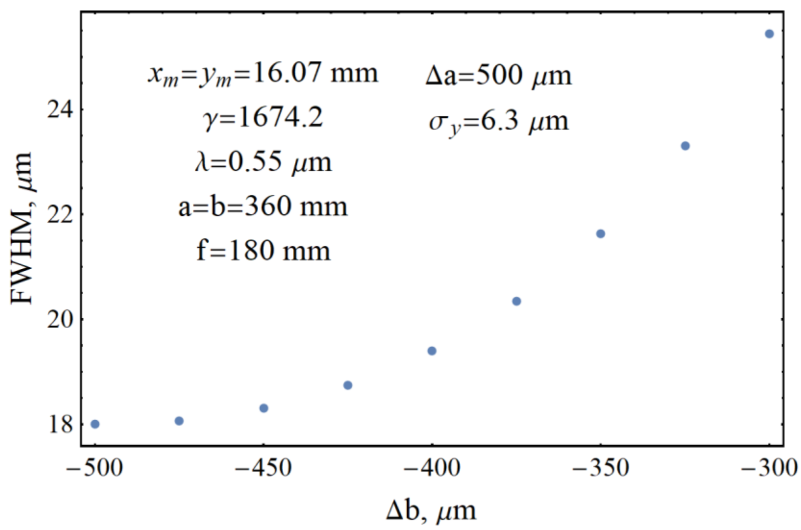

Fig. 17. Dependence between FWHM parameter of fitting functions and the positioning error values Δb

However, obtained dependences will only characterize the change of OTR shape in the region of positioning error values equal to $\Delta b = -500 ... -300$ μm and $\Delta a = 500$ μm.

As it was mentioned before, influence of non-ideal focusing conditions can be also assessed by the shift of maximum's position of PSF, if those are fitted by a specific function beforehand [11]:

$$f(y_i) = A \cdot y_i^2 \cdot \exp\left[-\frac{y_i^2}{B^2}\right], \quad (21)$$

where *A*, *B* are parameters of the fitting function which are defined automatically.

An example of such fitted PSF is shown in Figure 18.

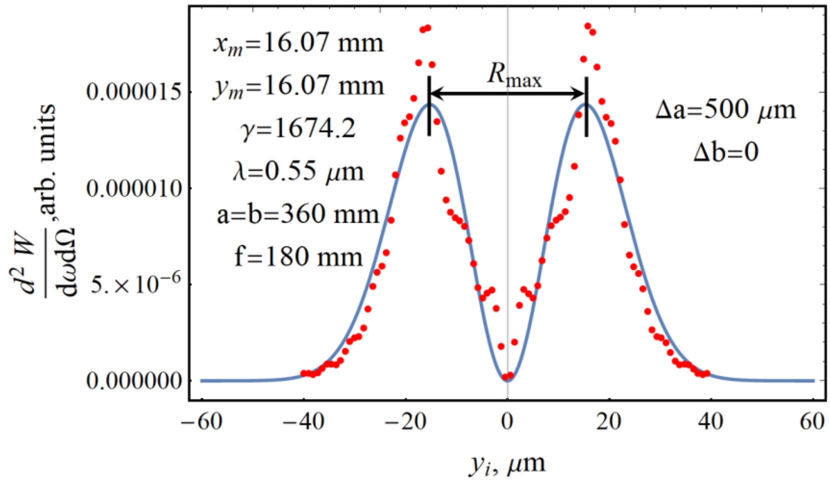

Fig. 18. An example of PSF being fitted by function (21) under non-ideal focusing conditions

Even though fitting function smoothes PSF distributions too much it still gives adequate representation of its characteristics. By using the distance between two maximums of PSF $R_{\max}$ for different sets of positioning error values one can obtain the following dependence (see Figure 19).

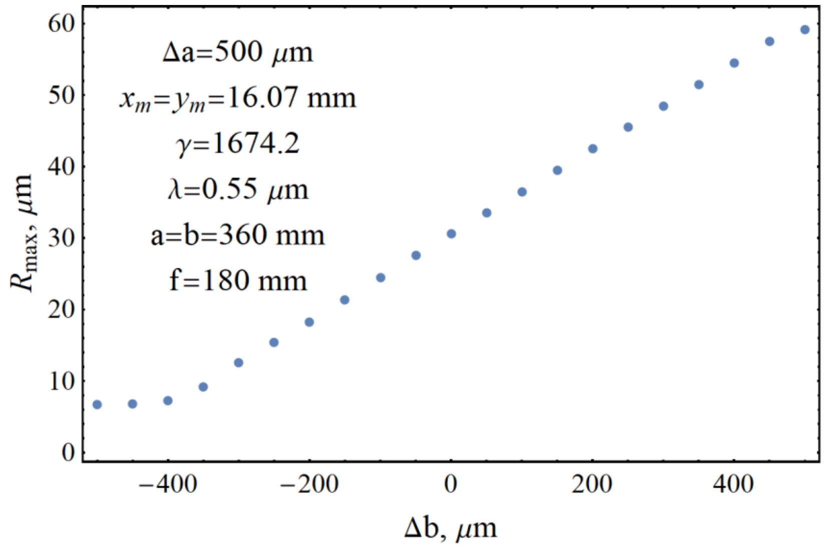

Fig. 19. Dependence between $R_{\max}$ parameter of fitting functions for PSFs and the positioning error values Δb

1.2.3 Chapter conclusion

The impact of non-ideal focusing conditions (i.e. lens displacement along optical axis) on the shape of OTR PFSs and intensity distributions from the whole electron bunch was studied through the simulation in the presented work. The dependence between distributions' parameters (FWHM and $R_{\max}$) and the values of positioning errors was determined by fitting original calculated data with specific fitting functions. Obtained results could be used to bring corrections to experimental data or optical system itself.

2 ODR for electron beam position monitoring purposes

2.1 Beam position monitor based on a rectangular slit

2.1.1 Model for simulation

ODR intensity distributions were calculated by using Wolfram Mathematica. For the sake of simplicity, only vertical polarization component of ODR in the case of horizontal slit is considered. The following electron beam parameters were chosen for calculation: γ = 2500, λ = 500 nm. Simulation scheme with all elements of optical system and target slit is shown in Figure 20.

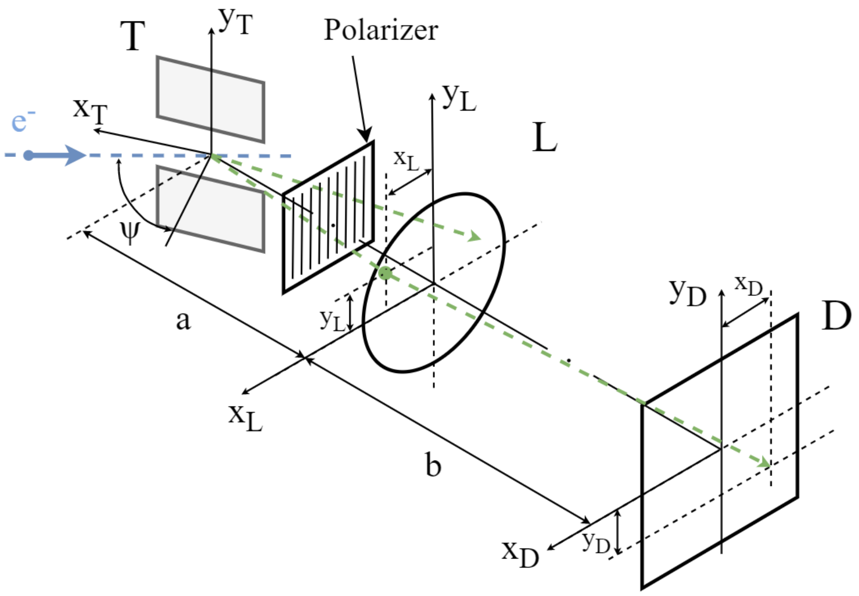

Fig. 20. Scheme of optical system for ODR focusing consisting of a target represented by a horizontal slit (T), a lens (L) and detector (D); Ψ – electron incident angle

Calculation for both polarization components of ODR field was carried out by the following formula [1]:

$$E^{D}_{\{x,y\}}(x_D, y_D) = const\int dx_T dy_T \frac{\{x_T, y_T\}}{\sqrt{x_T^{\,2}+y_T^{\,2}}}\times$$
$$\times K_1\left(\sqrt{x_T^{\,2}+y_T^{\,2}}\right)\exp\left[i\frac{x_T^2+y_T^2}{4\pi R}\right]\exp\left[-i\left(x_T x_L + y_T y_L\right)\right]\exp\left[-i\left(x_L\frac{x_D}{M}+y_L\frac{y_D}{M}\right)\right], \quad (22)$$

Following dimensionless units were used in the expression (22): $\{x_{T,D}, y_{T,D}\} = \frac{2\pi}{\gamma\lambda}\cdot\{X_{T,D}, Y_{T,D}\}$ are coordinates of the particle on the slit plane;

$\{x_L, y_L\} = \frac{\gamma}{a} \cdot \{X_L, Y_L\}$ are coordinates on the lens plane; $R = \frac{a}{\lambda\gamma^2} = 1$ is a parameter that characterizes far field wave zone [8]; M is the lens optical magnification; K_1 is the modified Bessel function.

In the case of a rectangular lens $(-x_m \le x_L \le x_m,\ -y_m \le y_L \le y_m)$ expression (22) can be simplified. Double integral for lens plane can be taken analytically [1]:

$$\int_{-x_m}^{x_m} dx_L \int_{-y_m}^{y_m} dy_L \exp\left[-i\left(x_T x_L + y_T y_L\right)\right] \exp\left[-i\left(x_L \frac{x_D}{M} + y_L \frac{y_D}{M}\right)\right] = \\ = \frac{4M^2 \sin\left[x_M\left(\frac{x_D}{M} + x_T\right)\right] \sin\left[y_M\left(\frac{y_D}{M} + y_T\right)\right]}{\left(x_D + M \cdot x_T\right)\left(y_D + M \cdot y_T\right)}, \tag{23}$$

where $\{x_M, y_M\} = \frac{\gamma}{a} \cdot \{X_M, Y_M\} = \{50, 50\}$ is a lens aperture.

Considering expression (23) one can rewrite expression (22) as follows:

$$E^D_{\{x,y\}}\left(x_D, y_D\right) = const \int dx_T dy_T \frac{\{x_T, y_T\} K_1\left(\sqrt{x_T^{\,2} + y_T^{\,2}}\right)}{\sqrt{x_T^{\,2} + y_T^{\,2}}} \times \\ \times \exp\left[i \frac{x_T^2 + y_T^2}{4\pi R}\right] \times \left(\frac{4M^2 \sin\left[x_M\left(\frac{x_D}{M} + x_T\right)\right] \sin\left[y_M\left(\frac{y_D}{M} + y_T\right)\right]}{\left(x_D + M \cdot x_T\right)\left(y_D + M \cdot y_T\right)}\right), \tag{24}$$

The region of integration for expression (24) is the following: $-5 < y_T < -h,\ h < y_T < 5,\ -5 < x_T < 5.$ Here, $h = \frac{2\pi}{\gamma\lambda} \cdot H$ is a half of the slit's width, H = 50 μm.

To obtain an expression for intensity distribution of ODR one should use the following expression:

$$I^D_{\{x,y\}}\left(x_D, y_D\right) = const\left|E^D_{\{x,y\}}\left(x_D, y_D\right)\right|^2. \tag{25}$$

2.1.2 Simulation results

Figure 21 shows an example of 2D ODR intensity distribution for both horizontal and vertical polarization components in the case when electron passes through the slit's center.

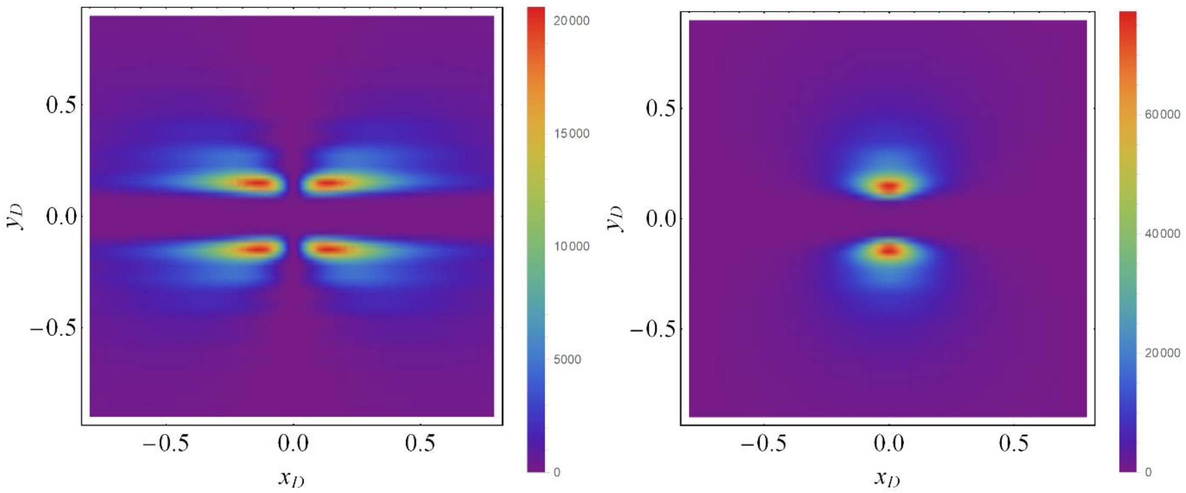

Fig. 21. 2D ODR intensity distribution for horizontal (on the left-hand side) and vertical polarization components (on the right-hand side). Horizontal slit's width is equal to 100 μm.

As can be seen from the Figure 21, it is better to use vertical polarization component as a source of electron's position information as it has only two maxima lying on $x_D = 0$, which simplifies the next task. To consider vertical offset of the incident electron, one should modify expression (24) as follows:

$$E_y^D(x_D, y_D, y_0) = const \int dx_T dy_T \frac{(y_T - y_0) K_1\left(\sqrt{x_T^{\ 2} + (y_T - y_0)^2}\right)}{\sqrt{x_T^{\ 2} + (y_T - y_0)^2}} \times$$
$$\times \exp\left[i \frac{x_T^2 + y_T^2}{4\pi R}\right] \times \left(\frac{4M^2 \sin\left[x_M\left(\frac{x_D}{M} + x_T\right)\right] \sin\left[y_M\left(\frac{y_D}{M} + y_T\right)\right]}{(x_D + M \cdot x_T)(y_D + M \cdot y_T)} \right), \tag{26}$$

where $y_0 = \frac{2\pi}{\gamma\lambda} \cdot Y_0$ is an offset of the incident electron along y-axis of the slit.

Intensity for that case is calculated the same way as in expression (25).

Figure 22 shows an example of ODR intensity distribution with violated symmetry in its peaks, which is induced by the vertical offset in electron's trajectory relative to the centre of the slit.

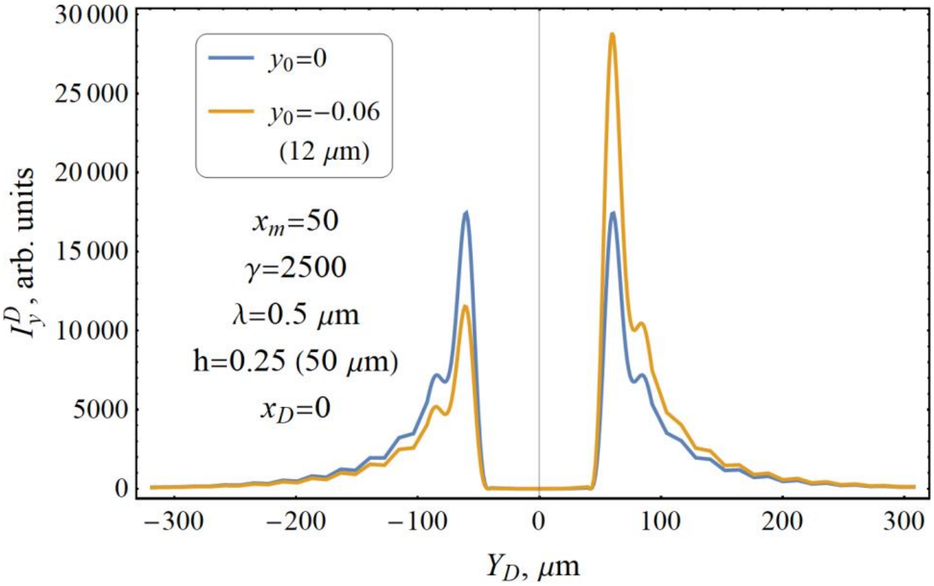

Fig. 22. Asymmetrical ODR intensity distribution of its vertical polarization component in the case of horizontal slit

Estimating the intensity ratio of main distribution peaks for different vertical positions of electron within the slit by using expression $\frac{I_{R\max} - I_{L\max}}{I_{R\max} + I_{L\max}}$, where $I_{R\max}$, $I_{L\max}$ are intensity values of right and left peak correspondingly, one can come up with such dependence that allows to determine the initial position of the particle within the slit plane at the moment it is crossed. An example of the mentioned dependence is presented in Figure 23.

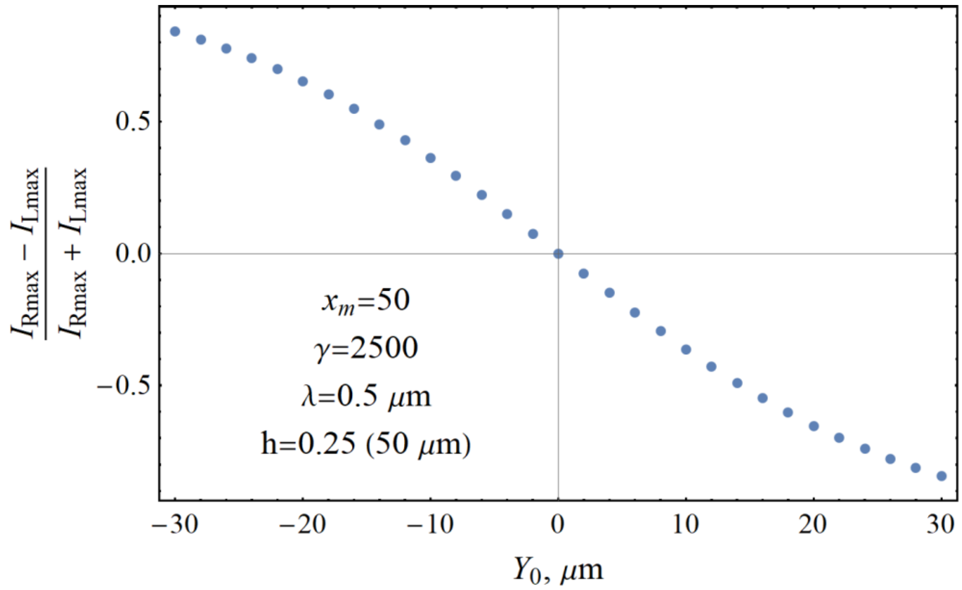

Fig. 23. Graph that reflects intensity ratio between two main distribution peaks on the initial electron's position along y-axis.

2.1.3 Chapter conclusion

The dependence that is shown in the current work allows to determine the initial vertical position of incident electron at the moment it crosses horizontal slit. However, to obtain horizontal position of the particle vertical slit should be applied. Despite the fact that the work only considers a single incident particle its results could be easily extrapolated with a good approximation on the electron beam passing through the slit whose width is greater than the beam size. Accuracy of the method suggested here depends on the accuracy in defining the position of distributions' peak intensity values (see Figure 22), which is determined by the wavelength of ODR and lens aperture, and, in the case mentioned above, does not exceed 5%.

2.2. Beam position monitor based on a circular aperture

2.2.1 Model for simulation

For the sake of simplicity, only vertical polarization component of ODR in the case of a circular aperture is considered. The following electron beam parameters were chosen for calculation: $\gamma = 2500$, $\lambda = 500$ nm. Simulation scheme with all elements of optical system and target slit is shown in Figure 24.

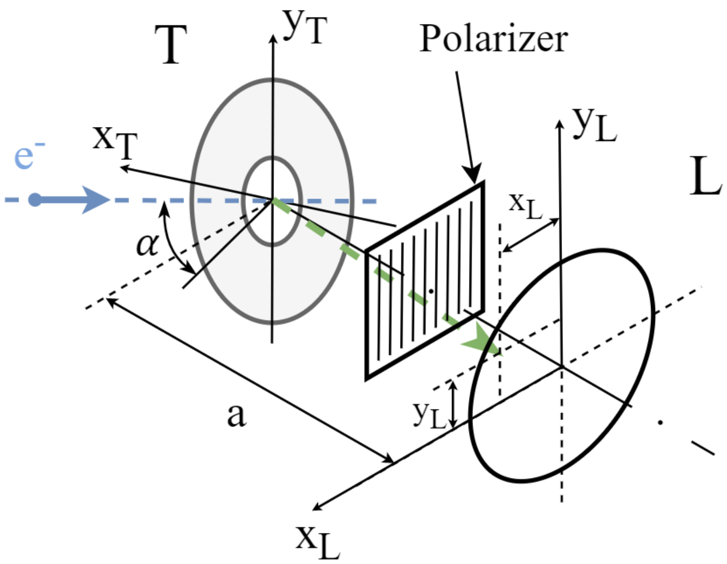

Fig. 24. Scheme of optical system for ODR focusing consisting of a target represented by a circular aperture (T) and a lens (L); α – electron incident angle

The formula that describes propagation of diffraction radiation in the case of normal incidence is the following [1]:

$$E_{x,y}^{L}\left(x_L, y_L\right) = const \int_0^{2\pi} d\varphi \int_h^{r_{\max}} dr_T \begin{Bmatrix} \cos\varphi \\ \sin\varphi \end{Bmatrix} r_T \frac{K_1\left(\rho\left(r_T\right)\right)}{\gamma} \exp\left[\frac{i}{4\pi R} r_T^2\right] \times \\ \times \exp\left[i\pi R\left(x_L^2 + y_L^2\right)\right] \times \exp\left[-i\left(r_T \cos\varphi x_L + r_T \sin\varphi y_L\right)\right] dr_T d\varphi, \quad (27)$$

here $\rho(r_T) = \sqrt{r_T^2 + x_0^2 + y_0^2 - 2r_T\sqrt{x_0^2 + y_0^2}\cos(\arctan(y_0 / x_0))}$, $R = \frac{a}{\lambda\gamma^2}$ is a parameter that characterizes far field wave zone [8], K_1 is the modified Bessel function, $\{x_0, y_0\} = \frac{2\pi}{\gamma\lambda} \cdot \{X_0, Y_0\}$ is an offset of the incident electron along corresponding axis of the circular aperture. The region of integration for expression above is the following:

$h < r_T < r_{T\max}$, $r_{T\max} = 5$ (1000 μm). Here $h = \frac{2\pi}{\gamma\lambda} \cdot H$ is a radius of the aperture, H = 50 μm.

Intensity is calculated in the same way as for previous chapters:

$$I_{x,y}^{L}\left(y_L, z_L\right) = const\left|E_{x,y}^{L}\left(x_L, y_L\right)\right|^2. \tag{28}$$

However, expressions (27) and (28) do not take into account the angle between the surface of the aperture and the incident particle. To check the effect of incident angle on simulation of ODR, one should use the following geometry shown in Figure 25.

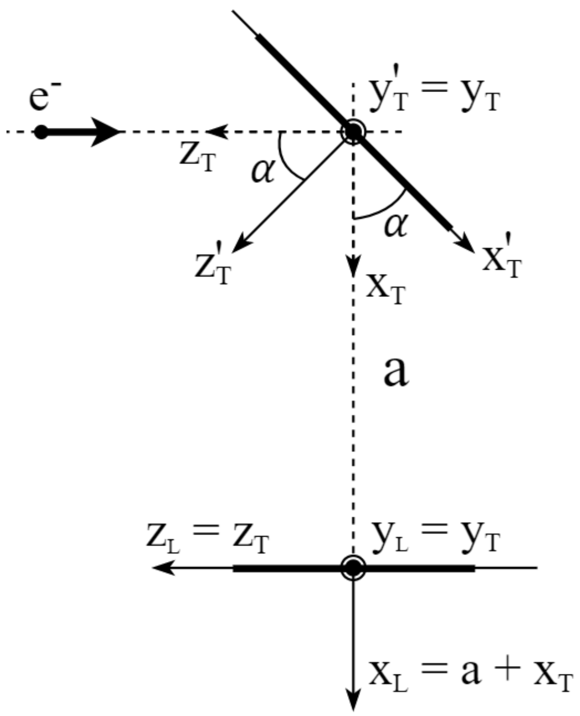

Fig. 25. Inclined target geometry for simulation of ODR from the circular aperture

In that case, the expression for the ODR field on the surface of the lens will take the following form after a couple of transformations according to new coordinate system of a tilted target with aperture:

$$E^L_{x,y}\left(y_L,z_L\right)=const\int_0^{2\pi}d\varphi\int_{h^*}^{r^*_{\max}}dr_T\begin{Bmatrix}\cos\varphi\\ \sin\varphi\end{Bmatrix}r_T\frac{K_1\left(\rho\left(r_T\right)\right)}{\gamma\cos\left(\alpha\right)}\times$$
$$\times\exp\left[\frac{i}{4\pi R}\left(r_T^2+r_T^2\cos^2(\varphi)\tan^2\right)\right]\exp\left[i\pi R\left(\left(\frac{r_T\cos\varphi}{2\pi R}+\gamma\right)^2+y_L^2+z_L^2\right)\right] \quad (29)$$
$$\times\exp\left[-i\left(r_T\cos\varphi\left(\frac{r_T\cos\varphi}{2\pi R}+\gamma\right)+r_T\sin\varphi y_L+\left(-r_T\cos\varphi\tan\alpha\right)z_L\right)\right],$$

where integration limits are expressed through ellipse equation: $h^*=\frac{h^2\cos(\alpha)}{\sqrt{(h\cos(\varphi))^2+(h\cos(\alpha)\sin(\varphi))^2}}$, $r^*_{\max}=\frac{r^2_{\max}\cos(\alpha)}{\sqrt{(r_{\max}\cos(\varphi))^2+(r_{\max}\cos(\alpha)\sin(\varphi))^2}}$.

ODR intensity distribution from the circular aperture can be calculated in the same manner as shown before:

$$I^L_{x,y}\left(y_L,z_L\right)=const\left|E^L_{x,y}\left(y_L,z_L\right)\right|^2. \quad (30)$$

2.2.2 Simulation results

Figure 26 shows how strong is the effect of tilted target on the ODR intensity distribution observed on the lens plane. Two cases are considered: when an electron experiences central incidence and when there is some offset between incident particle and the center of the aperture.

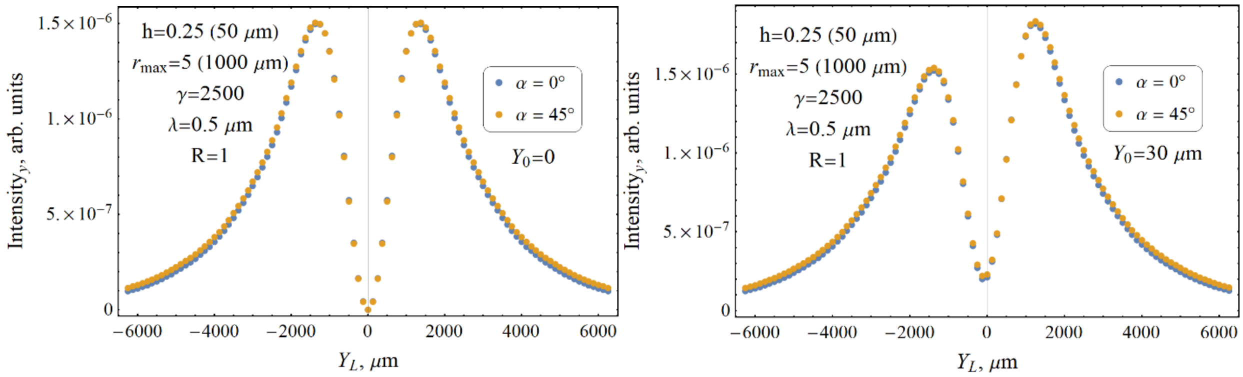

Fig. 26. Comparison of resulting ODR intensity distributions from the aperture with and without inclination; the one on the left-hand side is for central incidence case, the one on the right-hand side shows the changes in the presence of some offset

As one can notice there is almost no significant effect on the shape of distribution, and, actually, for high values of particle's Lorentz factor it has been expected to be extremely low.

In Figure 27 one can see comparison between central incidence and an incidence with some offset.

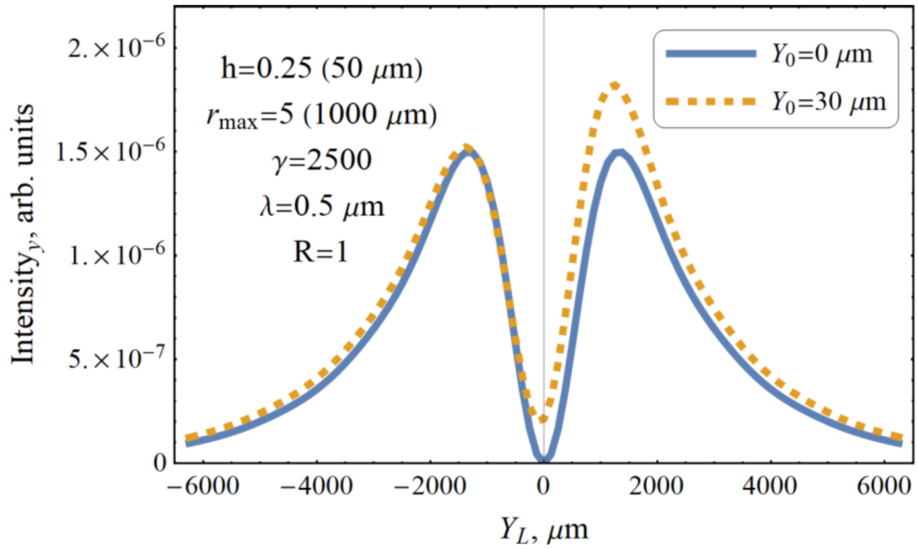

Fig. 27. The change in the shape of intensity distribution in the presence of some initial offset

It can be noticed, that only the symmetry is violated in the case of offset, but there is also a rise in central minimum.

To get the complete picture of the effect caused by the electron offset, 2D intensity distributions should be examined. Examples of such distributions are presented in Figure 28.

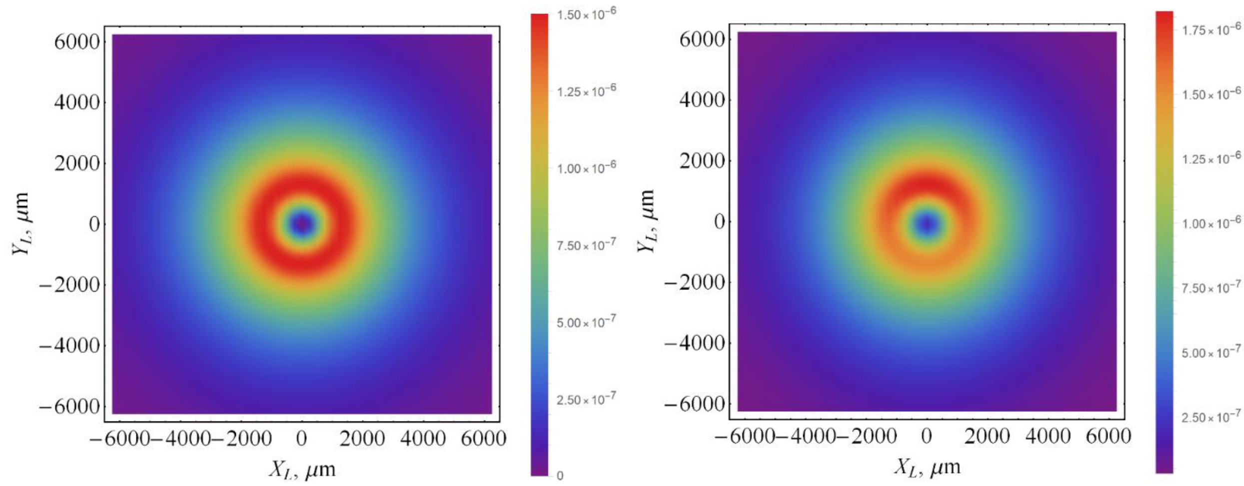

Fig. 28. 2D ODR intensity distributions for the circular aperture; on the left-hand size – central incidence, on the right-hand size – 30 μm offset along the y-axis

The right part of Figure 28 can be broken up into two polarization components to investigate the offset contribution for each polarization component (see Figure 29).

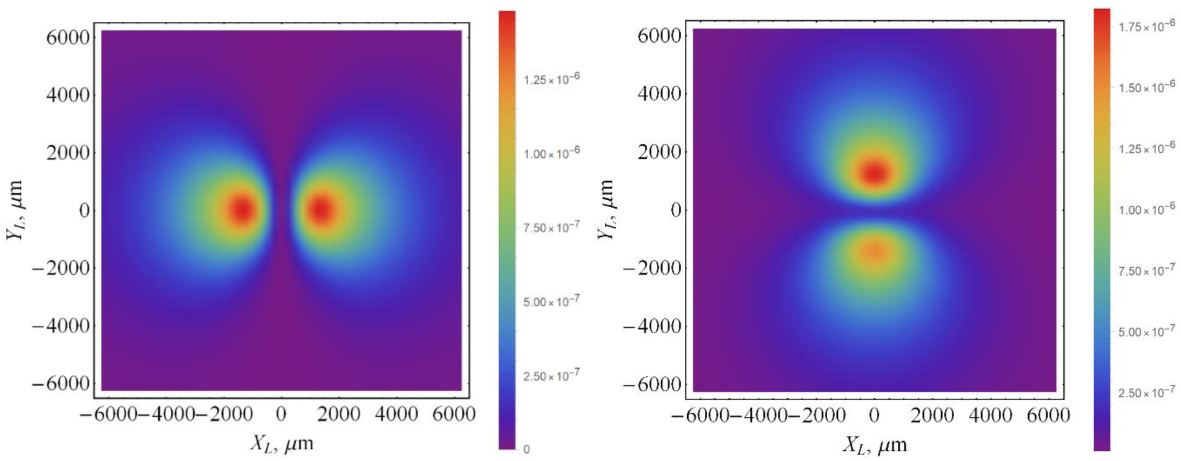

Fig. 29. 2D ODR intensity distribution for horizontal (on the left-hand side) and vertical (on the right-hand side) polarization components

It is clear that only vertical polarization component is affected if the offset is strictly along the corresponding axis. Now one can observe how the position of the peak intensity depends on the point where the electron crossed the aperture (see Figure 30).

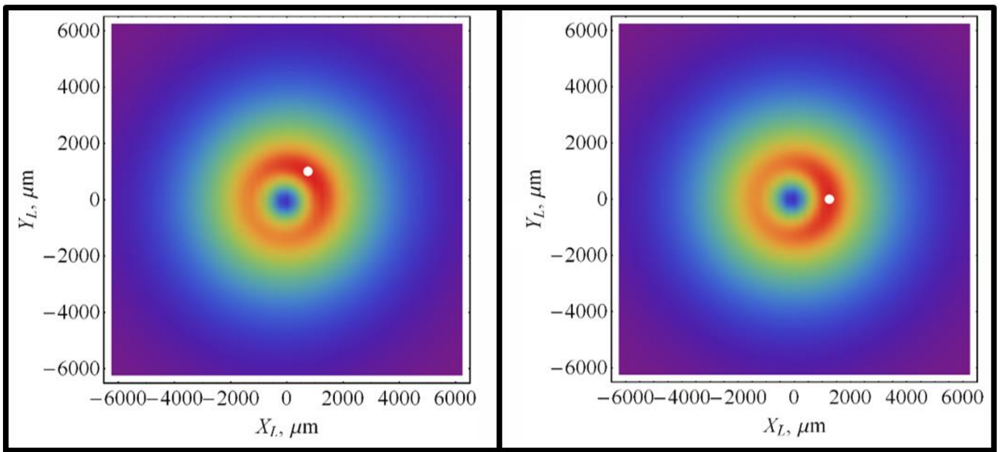

$X_0 = Y_0 = 30/\sqrt{2}\ \mu m$ Electron entering at φ = 45° Maximum at φ = 53°	$X_0 = 30\ \mu m$ Electron entering at φ = 0° Maximum at φ = 0°

Fig. 30. 2D ODR intensity distribution for polar angles equal to 45° (on the left-hand side) and 0° (on the right-hand side) at which the electron traverses the aperture; the maximum is marked with a white dot

As one can see from the Figure 30, it is possible to define the polar angle on the aperture plane at which the incident particle crosses that plane. As can be seen from the left part of Figure 30, maximum of intensity does not coincide with the polar angle of entry. Though this can be purely explained by the lack of points taken during the calculation process.

To obtain the distance between the point of incidence and the center of the aperture via these intensity patterns the parameter similar to the one from the previous chapter could be used: $\frac{I_{\text{MaxPeak}} - I_{\text{MinPeak}}}{I_{\text{MaxPeak}} + I_{\text{MinPeak}}}$. Results of such analysis is presented in Figure 31.

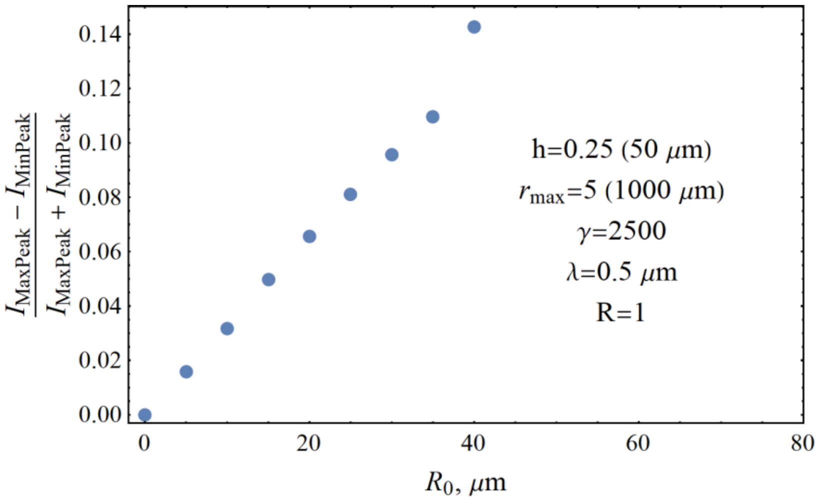

Fig. 31. Dependence between asymmetry in ODR intensity distribution and electron offset value; R_0 – is a distance between the incidence point of an electron and the center of the aperture

2.2.3 Chapter conclusion

Suggested method allows determining two coordinates of the incident electron at a time (unlike the method that involves rectangular slit).

Accuracy of the method suggested here depends on the accuracy in defining the position of distributions' peak intensity values, which is determined by the wavelength of ODR, and, in the case mentioned above, does not exceed 5%.

Intensity distributions observed in the work were calculated on a lens plane, therefore, to make method applicable for real-life cases those distributions should be additionally integrated throughout the lens plane to obtain images on the detector.

3 Financial management, resource efficiency and resource saving

The purpose of this section discusses the issues of competitiveness, resource efficiency, and resource-saving, as well as financial costs regarding the object of study of Master's thesis. Competitiveness analysis is carried out for this purpose. SWOT analysis helps to identify strengths, weaknesses, opportunities, and threats associated with the project, and give an idea of working with them in each particular case. For the development of the project requires funds that go to the salaries of project participants and the necessary equipment, a complete list is given in the relevant section. The calculation of the resource efficiency indicator helps to make a final assessment of the technical decision on individual criteria and in general.

3.1 Pre-project analysis

Nowadays the perspective of scientific research is determined not so much by the scale of discovery, which is difficult to estimate at the first stages of the life cycle of a high-tech and resource-efficient product, but by the commercial value of the development. Assessment of the commercial value of the development is a necessary condition when searching for sources of financing for scientific research and commercialization of its results. It is important for developers, who should represent the state and prospects of ongoing scientific research.

It is necessary to understand that the commercial attractiveness of scientific research is determined not only by the excess of technical parameters over previous developments but also by how quickly the developer will be able to find answers to such questions - whether the product will be in demand in the market, what will be its price, what is the budget of the scientific project, how long it will take to enter the market, etc.

The achievement of the goal is ensured by solving the tasks:

– evaluation of the commercial potential and prospects of scientific research;

– identifying possible alternatives to scientific research that meets current resource efficiency and resource conservation requirements;

– research planning;

– resource (resource-saving), financial, budgetary, social, and economic efficiency of research.

3.1.1 Competitiveness analysis of technical solutions

In order to find sources of financing for the project, it is necessary, first, to determine the commercial value of the work. It is important to realistically assess the strengths and weaknesses of competitor designs. Analysis of competitive technical solutions from the standpoint of resource efficiency and resource saving allows us to assess the comparative effectiveness of scientific development and determine the directions for its future improvement.

This analysis was carried out by using an evaluation card (Table 1). Two competitive developments were selected for this: the first one is beam diagnostic by using Faraday cup, the second one – by using luminophore screens. The criteria for comparing and evaluating resource efficiency and resource conservation, shown in Table 1, were selected based on the selected objects of comparison, taking into account their technical and economic features of development, creation and operation.

Evaluation map analysis presented in Table 1. The position of the research and competitors is evaluated for each indicator on a five-point scale, where 1 is the weakest position and 5 is the strongest. The weights of indicators determined in the amount are 1.

Analysis of competitive technical solutions is determined by the formula:

$$C = \sum W_i \cdot P_i; \qquad (31)$$

where C - the competitiveness of research or a competitor;

W_i – criterion weight;

P_i – point of i-th criteria;

$i1$ is for beam diagnostic by using Faraday cup;

$i2$ is for beam diagnostic by using luminophore screens.

This analysis suggests that the study is effective because it provides acceptable quality results. Further investment in this development can be considered reasonable.

Table 1 – Evaluation card for comparison of competitive technical solutions

Evaluation criteria	Criterion weight	Points			Competitiveness		
		P_f	P_{i1}	P_{i2}	C_f	C_{i1}	C_{i2}
1	2	3	4	5	6	7	8
Technical criteria for evaluating resource efficiency							
1. Informativeness of the applied method	0.2	5	5	3	1	1	0.6
2. Accuracy of received beam profile data	0.06	4	4	4	0.24	0.24	0.24
3. Influence on the measured object	0.1	4	5	2	0.4	0.5	0.2
4. Requirement for detecting device	0.02	4	2	3	0.08	0.04	0.06
5. Feasibility of online data processing	0.1	4	3	5	0.4	0.3	0.5
6. Easy to use	0.05	5	3	3	0.25	0.15	0.15
7. Availability of expensive equipment	0.1	5	3	3	0.5	0.3	0.3
Economic criteria for performance evaluation							
1. Development cost	0.1	3	4	4	0.3	0.4	0.4
2. Product competitiveness	0.04	4	3	3	0.16	0.12	0.12
3. Popularity of the method	0.03	4	4	4	0.12	0.12	0.12
4. Interest in scientific development	0.2	5	2	2	1	0.4	0.4
Total	1				4.45	3.57	3.09

3.1.2 SWOT analysis

Complex analysis solution with the greatest competitiveness is carried out with the method of the SWOT analysis: Strengths,Weaknesses, Opportunities and Threats. The analysis has several stages. The first stage consists of describing the strengths and weaknesses of the project, identifying opportunities and threats to the project that have emerged or may appear in its external environment. The second stage consists of identifying the compatibility of the strengths and weaknesses of the project with the external environmental conditions. This compatibility or incompatibility should help to identify what strategic changes are needed.

The SWOT analysis of this research project is presented in Table 2.

Table 2 – SWOT matrix

	Strengths: S1: Almost no influence on the object of measurements S2: High performance	**Weaknesses:** W1: A need for developing of individual scheme for each acceleration set-up
Opportunities: O1: Expansion of opportunities for electron beam diagnostic purposes	Analysis results of interactive matrix fields "Strengths and opportunities": 1. Feasibility of developing relatively cheap schemes for electron beam diagnostic with advanced beam parameters 2. Gathering and analysis of obtained data will allow enhancement of data treatment algorithm	Analysis results of interactive matrix fields "Weakness and opportunities": 1. Development of a typical scheme for diagnostics, designed for the widest possible range of equipment 2. Increase calculation power to increase the amount of data treated
Threats: T1: Lack of funding from the government and private business T2: Backlog of researches in associated areas T3: Lack of specialists with corresponding qualification	Analysis results of interactive matrix fields "Strengths and threats": 1. Presenting of research outcomes in scientific society	Analysis results of interactive matrix fields "weakness and threats": 1. Obtaining grants and fundings for researches

Based on the results of the analysis of this matrix, it can be concluded that the difficulties and challenges that this research project may face in one way or another can be addressed by the existing strengths of the research.

3.2 Project initiation

The initiation process group consists of processes that are performed to define a new project or a new phase of an existing one. In the initiation processes, the initial purpose and content are determined and the initial financial resources are fixed. The internal and external stakeholders of the project who will interact and influence the overall result of the research project are determined.

3.2.1 Project objectives and results

This section describes the project stakeholders, the hierarchy of project objectives and the criteria for achieving the objectives.

Project stakeholders refer to individuals or organisations that are actively involved in the project or whose interests may be affected positively or negatively during project implementation or completion. Information on project stakeholders shows in Table 3.

Table 3 – Stakeholders of the project

Project stakeholders	**Stakeholder expectations**
Research centers with linear electron accelerators	Advanced high-precision electron beam diagnostic method that allows online beam monitoring to assure beam quality and stability
Medical centers with advanced μCT devices	Advanced high-precision electron beam diagnostic method that allows online beam monitoring to provide such quality of the beam that will meet requirements for high-quality μCT imaging

Table 4 shows information on the hierarchy of project objectives and criteria for achieving the objectives.

Table 4 – Purpose and results of the project

Purpose of the project	To develop high-precision non-invasive electron beam diagnostic method based on optical transition and diffraction radiation for beam transverse size measurements and position monitoring.
Expected results of the project	1. Method for measuring electron bunch transverse size via coherent optical transition radiation. 2. Method for electron beam position monitoring via optical diffraction radiation based on a rectangular slit and circular aperture
Criteria for acceptance of the project result	1. Transverse bunch size measurements with less than 10 μm resolution. 2. Error in defining beam position should not exceed 5%.
Requirements for the project result	1. Dependences that can be used to define transverse electron beam size by analyzing intensity distribution patterns of OTR on the detector plane. 2. Dependences that can be used to define initial position of the electron beam within a slit or aperture at the moment it crosses target plane by analyzing intensity distribution patterns of ODR on the detector plane. 3. The research carried out under this project should be completed by June 4, 2021. 4. The results obtained must meet the criteria for accepting the project result.

3.2.2 The organizational structure of the project

At this stage of the work, it was necessary to solve the following questions: who will be a member of the working group of the given project, to define the role of each participant in the given project, and also to prescribe the functions carried out by each of the participants and their labor input in the project. This information is presented in tabular form (see Table 5).

Table 5 – Project working group

№	**Participant**	**Role in the project**	**Functions**	**Labour time, hours**
1	Alexander P. Potylitsyn, D.Sc. of Physics Sciences, Professor, TPU	Supervisor	Responsible for the project implementation within the set resource constraints, coordinates the activities of the project participant.	750
2	Gusvitskii Todor, Master, TPU	Executor	Review of literary sources and technical literature; calculation of COTR, OTR, ODR intensity distributions; writing the master's thesis	100
Total				850

3.2.3 Limitations and assumptions of the project

Project restrictions are all factors that may serve to limit the degree of freedom of the project team members, as well as "project boundaries" - parameters of the project or its product that will not be implemented within the project. Table 6 shows the main limitations of this work.

Table 6 – Project limitations

Factors	**Limitations/Assumptions**
1. Project budget	153695 RUB
1.1 Source of financing	TPU funding
2. Project time limits	27.01.2021 – 01.06.2021
2.1 Date of project management plan approval	03.02.2021
2.2 Project completion date	01.06.2021
3. Other restrictions and assumptions	Epidemiological situation (Coronovirus)

3.3 Scientific research planning

The Graduate Qualification Study (GQR) is a work of a scientific nature related to scientific inquiry, research to obtain scientific generalizations, to find principles and ways of creating (modernizing) products, it includes:

1. fundamental research carried out with a view to enhancing scientific knowledge, phenomena and patterns of their development without regard to their specific practical application;

2. search research carried out with the purpose of finding ways to use the revealed phenomena and regularities in a concrete field of science and technology for creation of principally new products, materials and technologies;

3. applied research aimed at solving scientific problems, improvement of methods in order to obtain specific results used in experimental and design developments in the creation of scientific and technical.

3.3.1 Structure of work within the scientific research

Planning of the complex of proposed works is carried out in the following order:

- determination of the structure of works within the scientific research;
- definition of participants of each work;
- determination of the duration of work;
- construction of the schedule for scientific research.

To carry out scientific research, a working group is formed, which may include researchers and teachers, engineers, technicians, and laboratory technicians, the number of groups may vary. For each type of work to be carried out, an appropriate position for the executors shall be established. In this section, it is necessary to make a list of stages and works within the framework of scientific research, to make a distribution of performers by type of work. An approximate order of drawing up stages and works, distribution of performers by these types of work is shown in Table 7.

The table contains a list of the main stages of the study, the work performed in the study, and the distribution of roles of the work performers.

3.3.2 Development of a schedule for scientific research

During the performance of the thesis, for convenience and clarity, a ribbon schedule of scientific works is constructed in the form of a Gantt chart. The works on the topic are presented as long sections of time, characterized by the start and end dates of these works.

For the convenience of drawing a chart, the duration of each stage of work should be translated from working days to calendar days. To do this, you are should use the following formula:

$$T_{Ki} = T_{Pi} \cdot k_{cal}, \qquad (32)$$

where T_{Ki} – the duration of the i-th job in calendar days; T_{Pi} – duration of the i-th job in working days; k_{cal} – calendar factor.

Table 7 – List of stages, works and distribution of performers

№	Contents of work	Executor's position
1	Drawing up the technical assignment	Supervisor, Executor
2	Literature review	Executor
3	Selection of the method’s general idea and design of the experiment	Supervisor, Executor
4	Calendar planning	Supervisor, Executor
5	Calculations algorithm design and preliminary calculations and justifications	Executor
6	ODR/OTR field calculations (lens)	Executor
7	ODR/OTR field calculations (detector)	Executor
8	ODR/OTR intensity calculations (detector)	Executor
9	Defining the dependence of intensity distributions on position and size of the electron bunch	Executor
10	Analysis of the results	Executor
11	Evaluation of the effectiveness of the results	Supervisor, Executor
12	Drawing up a final report	Executor
13	Preparing to defend a diploma thesis	Supervisor, Executor

The coefficient of calendar is determined by the following formula:

$$k_{cal} = \frac{T_{cal}}{T_{cal} - T_{weekend} - T_{hol}} = \frac{366}{366 - 52 - 14} = 1.22; \quad (33)$$

where T_{cal} – calendar day per year; $T_{weekend}$ – a number of days off per year; T_{hol} – a number of holidays per year.

All calculated values are summarized in Table 8.

On the basis of Table 8, a time schedule is constructed (see Table 9). The schedule is constructed for the maximum duration of the research project by months and decades (10 days) for the period of writing the diploma. At the same time, the works on the schedule should be distinguished by different shading depending on the executors responsible for this or that work.

Table 8 – A project timeline in working days

Task	The laboriousness of the task						Duration of the task in working days T_{pi}		Duration of the task in calendar days $T_{\kappa i}$	
	t_{min}, person-days		t_{max}, person-days		t_{expi}, person-days					
	Supervisor	Executor	Supervisor	Executor	Supervisor	Executor	Supervisor	Executor	Supervisor	Executor
Drawing up the technical assignment	3		8		5		5		7	
Literature review		4		9		6		6		9
Selection of the method's general idea and design of the experiment		5		8		6		6		9
Calendar planning	10		15		12		6		9	
Calculations algorithm design and preliminary calculations and justifications		5		10		7		7		10
ODR/OTR field calculations (lens)		1		2		1		1		1
ODR/OTR field calculations (detector)		2		3		2		2		3
ODR/OTR intensity calculations (detector)		4		5		4		4		6
Defining the dependence of intensity distributions on position and size of the electron bunch		1		2		1		1		1
Analysis of the results		5		9		6		3		4
Evaluation of the effectiveness of the results		3		4		3		3		4
Drawing up a final report	6		10		8		4		6	
Preparing to defend a diploma thesis		6		10		10		10		15

Table 9 – Calendar plan-graph in the form of a Gantt chart

№	Task	Participants	$T_{\kappa i}$ days	Duration of the task																				
				January				February				March				April					May			
				1	2	3	4	1	2	3	4	1	2	3	4	1	2	3	4	5	1	2	3	4
1	Drawing up the technical assignment	Supervisor	3																					
2	Literature review	Executor	5																					
3	Selection of the method's general idea and design of the experiment	Executor	9																					
4	Calendar planning	Supervisor	1																					
5	Calculations algorithm design and preliminary calculations and justifications	Executor	10																					
6	ODR/OTR field calculations (lens)	Executor	5																					
7	ODR/OTR field calculations (detector)	Executor	10																					
8	ODR/OTR intensity calculations (detector)	Executor	10																					
9	Defining the dependence of intensity distributions on position and size of the electron bunch	Executor	10																					
10	Analysis of the results	Executor	7																					
11	Evaluation of the effectiveness of the results	Executor	5																					
12	Drawing up a final report	Supervisor	5																					
13	Preparing to defend a diploma thesis	Executor	10																					

– Executor   – Supervisor

3.4 Scientific and technical research budget

The amount of costs associated with the implementation of this work is the basis for the formation of the project budget. This budget will be presented as the lower limit of project costs when forming a contract with the customer.

To form the final cost value, all calculated costs for individual items related to the manager and the student are summed.

In the process of budgeting, the following grouping of costs by items is used:

– material costs of scientific and technical research;

– costs of special equipment for scientific work (Depreciation of equipment used for design);

– basic salary;

– additional salary;

– labor tax;

– overhead.

3.4.1 Material cost calculation

This item includes the cost of purchasing all types of materials, components, and semi-finished products required to perform work on the subject. Calculation of the cost of material expenses is made at current price lists or contractual prices. The results of this cost item are recorded in Table 10.

Table 10 – Costs of materials

Name	Unit of measurement	Number	Price per unit, RUB	Expenses (E_M), RUB
Paper	Pack	1	250	250
Pens	Unit	2	50	100
Pencils	Unit	1	50	50
Ruler	Unit	1	40	40
Printing	Page	200	2	400
Folder	Unit	2	5	10
Stapler	Unit	1	150	150
Staples	Pack	1	40	40
Hole puncher	Unit	1	250	250
Total				**1 290**

3.4.2 Calculation of equipment costs

Table 11 – Calculation of the budget of expenses for equipment for scientific works

№	Name	Num ber	Price per unit, RUB	Total price of equipment, RUB
1	Laptop	1	35 000	35 000
2	Microsoft Windows 10 Professional RU x64	1	4 000	4 000
3	Wolfram Mathematica	1	7 498	7 498
4	Microsoft Office 2019 Home and Student	1	2 500	2 500
Total, RUB				**48 998**

The cost of specialized equipment is recorded in the form of depreciation charges.

Depreciation is the gradual transfer of costs incurred to purchase or build property, plant and equipment to the cost of the finished product. With its help, money spent on the construction or purchase of property is compensated. Depreciation deductions are paid during the entire period of property exploitation.

Let's calculate the amount of monthly depreciation deductions in a linear way. Equipment costs are 48 998 RUB. The operating life of the computer is 7 years, the

Microsoft Windows 10 license is 4 years, the rest of the software is a year. Then the annual depreciation rate for them, respectively:

$$N_{D,Lap} = \frac{1}{7} \cdot 100\% = 14.29\%, \quad (34)$$

$$N_{D,Win} = \frac{1}{4} \cdot 100\% = 25\%, \quad (35)$$

$$N_{D,SS} = \frac{1}{1} \cdot 100\% = 14.29\%. \quad (36)$$

Academic year depreciation (9 months) for Laptop, Microsoft Windows 10 License, and Supporting Software:

$$D_{Lap} = 35000 \cdot \frac{N_{D,Lap}}{100\%} \cdot \frac{T}{365} = 35000 \cdot \frac{14.29\%}{100\%} \cdot \frac{90}{365} = 1233.2 \text{ RUB}, \quad (37)$$

$$D_{Win} = 4000 \cdot \frac{N_{D,Win}}{100\%} \cdot \frac{T}{365} = 4000 \cdot \frac{25\%}{100\%} \cdot \frac{90}{365} = 246.6 \text{ RUB}, \quad (38)$$

$$D_{SS} = 9998 \cdot \frac{N_{D,SS}}{100\%} \cdot \frac{T}{365} = 9998 \cdot \frac{100\%}{100\%} \cdot \frac{90}{365} = 2465.3 \text{ RUB}, \quad (39)$$

where T – number of working days.

Total depreciation for a year:

$$D = 3945.1 \text{ RUB}. \quad (40)$$

3.4.3 Basic and additional salary

This point includes the amount of payments stipulated by the legislation on labor, for example, payment of regular and additional holidays; payment of time associated with state and public duties; payment for work experience, etc.

This point includes the basic salary of participants directly involved in the implementation of work on this research. The value of salary costs is determined based on the labor intensity of the work performed and the current salary system.

The basic salary (S_{base}) is calculated according to the following formula:

$$S_{base} = S_{day} \cdot T_w, \quad (41)$$

where S_{day} – an average daily salary of an participant, rub; T_w – a duration of the work performed by the scientific and technical worker, working days.

The average daily salary (S_{day}) is calculated by the formula:

$$S_{day} = \frac{S_{month} \cdot M}{F_V}, \tag{42}$$

where S_{month} – a monthly salary of an participant, rub.; M – the number of months of work without leave during the year; F_V – valid annual fund of working time of scientific and technical personnel (251 days).

The number of months of work without vacation during the year is calculated as follows: at 24 working days of vacation M = 11.2 months, 5-day week. Table 12 calculates the actual annual fund of scientific and technical staff.

Table 12 – The valid annual fund of working time

Working time indicators	**Supervisor**	**Student**
Calendar number of days	366	366
The number of non-working days – weekend – holidays	 52 14	 52 14
Loss of working time – vacation – sick absence	 48 0	 48 0
The valid annual fund of working time	252	252

Monthly salary is calculated by formula:

$$S_{month} = S_{base} \cdot \left(k_{premium} + k_{bonus}\right) \cdot k_{reg}, \tag{43}$$

where $k_{premium}$ – premium rate; k_{reg} – regional rate; k_{bonus} – bonus rate.

Table 13 below calculates the base salary of the supervisors, the consultant, and the executor.

Additional salary include the amount of payments stipulated by the legislation on labor, for example, payment of regular and additional holidays; payment of time associated with state and public duties; payment for work experience, etc.

Additional salaries (S_{add}) are calculated on the basis of 10-15% of the base salary of workers:

$$S_{add} = S_{base} \cdot k_{extra}, \quad (44)$$

where k_{extra} – additional salary coefficient (10%); S_{base} – base salary, rubles.

Table 13 – Calculation of the basic salary

Performers	**Salary, rub**	k_{reg}	S_{month}**, rub**	S_{day}**, rub**	T_w**, work-days**	S_{base}**, rub**
Supervisor	33775	1.3	43907.5	1959.2	15	29388.3
Executor	17000	1.3	22100	986.1	43	42403.8

The additional salaries are equal to:

1) Supervisor:

$$S_{add} = S_{base} \cdot k_{extra} = 29388.3 \cdot 0.1 = 2938.8 \text{ RUB}. \quad (45)$$

2) Executor:

$$S_{add} = S_{base} \cdot k_{extra} = 42403.8 \cdot 0.1 = 4240.4 \text{ RUB}. \quad (46)$$

3.4.4 Labour tax

Tax to extra-budgetary funds is compulsory according to the norms established by the legislation of the Russian Federation to the state social insurance (SIF), pension fund (PF), and medical insurance (FCMIF) from the costs of workers.

Payment to extra-budgetary funds is determined of the formula:

$$P_{social} = k_b \cdot \left(S_{base} + S_{add}\right), \quad (47)$$

where k_b – coefficient of deductions for labor tax.

In accordance with the Federal law of July 24, 2009 No. 212-FL, the amount of insurance contributions is set at 30%. Institutions conducting educational and scientific activities have rate - 27.1%.

The labor tax is presented in Table 14.

Table 14 – Labor tax

Performers	Supervisor	Executor
Coefficient of deductions	0.271	
Salary, rub	32327.1	46644.2
Labour tax, rub	8760.6	12640.6
Total, rub	21401.2	

3.4.5 Overhead costs

Overhead costs include other management and maintenance costs that can be allocated directly to the project. In addition, this includes expenses for the maintenance, operation and repair of equipment, production tools and equipment, buildings, structures, etc.

The work was performed using a stationary computer with an average power of 550W(0.55 kW). If we assume that all the work was done on it, then everything was spent:

$$E = P \cdot F_{sum} = 0.55 \cdot 292 = 160.6 \text{ kW} \cdot \text{h}, \qquad (48)$$

where P – equipment power is measured in kW; F_{sum} – time of use of the equipment in hours.

Electricity costs are calculated using a formula:

$$C_{el} = T_{el} \cdot E = 10.18 \cdot 160.6 = 1634.91 \text{ RUB}, \qquad (49)$$

where T_{el} – tariff for industrial electricity (10.18 rubles per 1 kW·h).

A month of Internet use costs 350 rubles, in this work Internet was used for 4 months, so the cost of the Internet was 1400 rubles.

The overhead costs in this work amounted to 3034.91 RUB.

3.5 Formation of budget costs

The calculated amount of research and development work costs is the basis for forming the project cost budget. The definition of the research project cost budget for each option is given in Table 15.

Table 15 – The budget for scientific and technical research

Name of expenditure items	Cost, rubles
Material costs	1 290
Costs of special equipment	48 998
Basic salary	71792.1
Additional salary	7179.2
Labor tax	21401.2
Overhead	3034.91
Total planned cost	153695.4

3.6 Project risk register

Identified project risks include possible undefined events that may occur in the project and cause unintended consequences. Information on this section is presented in Table 16.

Table 16 – Register of risks

№	Risk	Potential effects	Proba-bility (1-5)	Effect of risk (1-5)	Level of risk	Ways to mitigate risk	Conditions of occurrence
1	Break down of a computer	Impossibility of conducting simulation	2	5	High	Technical maintenance	Improper handling of a computer
2	Mismatch of data received with expected results	Failure to meet project objectives	3	2	Low	Better analysis of literary sources	Error in predicting expected results

3.7 Determining research resource efficiency

Determination of efficiency is based on the calculation of the integral indicator of scientific research efficiency. Its location is related to the definition of two weighted average values: financial efficiency and resource efficiency.

The integrated indicator of resource efficiency of variants of execution of the object of research can be defined as follows:

$$I_{pi} = \sum a_i \cdot b_i, \qquad (50)$$

where I_{pi} – integral resource efficiency index for the i-th variant of development execution; a_i – development weighting factor; b_i^a, b_i^b – an evaluation of the i-th variant of the development's execution is set by the expert by the selected evaluation scale.

The calculation of the integral resource efficiency index of this study is presented in the form of Table 17.

Table 17 – Comparative assessment of the characteristics of the project implementation options

Criteria	**Parameter weighting factor**	**Current project**	**Analog 1**	**Analog 2**
Helps to increase user productivity	0.1	5	4	2
Convenient operation (meets customer requirements)	0.15	4	5	3
Interference immunity	0.15	4	4	2
Energy saving	0.2	5	4	3
Reliability	0.25	4	4	4
Material capacity	0.15	4	3	4
Total	1	4.3	4	3.15

An integrated financial indicator for development is defined as:

$$I_f^p = \frac{F_i}{F_{\max}}, \qquad (51)$$

where F_i – a cost of the i-th option; F_{max} – a maximum cost of execution of the scientific and technical research (including analogues).

$$I_f^p = \frac{F_p}{F_{\max}} = \frac{153695.4}{160099} = 0.96, \quad (52)$$

$$I_f^{a1} = \frac{F_{a1}}{F_{\max}} = \frac{156897}{160099} = 0.98, \quad (53)$$

$$I_f^{a2} = \frac{F_{a2}}{F_{\max}} = \frac{160099}{160099} = 1, \quad (54)$$

The integrated index of efficiency of development variants (I_{fin}^p) and analogues (I_{fin}^a) is determined on the basis of the integrated index of resource efficiency and integrated financial index by formulas:

$$I_{fin}^p = \frac{I_m^p}{I_f^p} = \frac{4.3}{0.96} = 4.43, \quad (55)$$

$$I_{fin}^{a1} = \frac{I_m^{a1}}{I_f^{a1}} = \frac{4}{0.98} = 4.06, \quad (56)$$

$$I_{fin}^{a2} = \frac{I_m^{a2}}{I_f^{a2}} = \frac{3.15}{1} = 3.15, \quad (57)$$

Comparison of the integral performance indicator of the current project and its analogues will allow to determine the comparative efficiency of the project (see Table 18).

Comparative effectiveness of the project:

$$C_{Eff} = \frac{I_{fin}^p}{I_m^p}. \quad (58)$$

Based on the calculation of the integral indicator with the definition of two weighted average values: financial efficiency and resource efficiency of scientific research, we can conclude that the comparative assessment of the current project is higher than other analogs.

Table 18 – Comparative development efficiency

Indicators	Current project	Analog 1	Analog 2
Integral resource efficiency indicator	4.3	4	3.15
Integral performance indicator for variants	4.43	4.06	3.15
Comparative performance of the variants	1.04	1.01	1

Thus, in this section was developed stages for design and creation competitive developed that meet the requirements in the field of resource efficiency and resourcesaving.

3.8 Conclusions under financial management

These stages include:

– development of a common economic project idea, the formation of a project concept;

– organization of work on a research project;

– identification of possible research alternatives;

– research planning;

– assessing the commercial potential and prospects of scientific research from the standpoint of resource efficiency and resource-saving;

– determination of resource (resource-saving), financial, budget, social, and economic efficiency of the project.

In the course of performing the economic part of the diploma work, calculations were made of the planned cost of research and the time spent.

The total cost of work is 153695.4 RUB, the main component of which is the cost of wages to perform scientific and technical research. The time required to perform the work was 84 calendar days.

4 Social responsibility

4.1 Introduction

Research work that was carried out in the current paper is dedicated to electron beam diagnostics including transverse size measurement and beam position monitoring via optical transition radiation and optical diffraction radiation. It comprises simulation of OTR and ODR intensity distributions and the result obtained here is represented by dependences which can be used to estimate electron beam parameters in real-life experiments on advanced accelerators.

Potential users of the project are research centers with modern electron linear accelerators that are used to study the biochemical processes that occur with protein radiopharmaceutical vehicles inside human body or advanced medical centers, where some of electron accelerators are used for μCT angiography.

4.2 Legal and organizational items in providing safety

Nowadays one of the main ways to radical improvement of all prophylactic work referred to reduce Total Incidents Rate and occupational morbidity is the widespread implementation of an integrated Occupational Safety and Health management system. That means combining isolated activities into a single system of targeted actions at all levels and stages of the production process.

Occupational safety is a system of legislative, socio-economic, organizational, technological, hygienic and therapeutic and prophylactic measures and tools that ensure the safety, preservation of health and human performance in the work process [12].

According to the Labor Code of the Russian Federation, every employee has the right:

- to have a workplace that meets Occupational safety requirements;
- to have a compulsory social insurance against accidents at manufacturing and occupational diseases;

- to receive reliable information from the employer, relevant government bodies and public organizations on conditions and Occupational safety at the workplace, about the existing risk of damage to health, as well as measures to protect against harmful and (or) hazardous factors;

- to refuse carrying out work in case of danger to his life and health due to violation of Occupational safety requirements;

- be provided with personal and collective protective equipment in compliance with Occupational safety requirements at the expense of the employer;

- for training in safe work methods and techniques at the expense of the employer;

- for personal participation or participation through their representatives in consideration of issues related to ensuring safe working conditions in his workplace, and in the investigation of the accident with him at work or occupational disease;

- for extraordinary medical examination in accordance with medical recommendations with preservation of his place of work (position) and secondary earnings during the passage of the specified medical examination;

- for warranties and compensation established in accordance with this Code, collective agreement, agreement, local regulatory an act, an employment contract, if he is engaged in work with harmful and (or) hazardous working conditions.

The labor code of the Russian Federation states that normal working hours may not exceed 40 hours per week, The employer must keep track of the time worked by each employee.

Rules for labor protection and safety measures are introduced in order to prevent accidents, ensure safe working conditions for workers and are mandatory for workers, managers, engineers and technicians.

4.3 Basic ergonomic requirements for the correct location and arrangement of researcher's workplace

The workplace when working with a PC should be at least 6 square meters. The legroom should correspond to the following parameters: the legroom height is at least 600 mm, the seat distance to the lower edge of the working surface is at least 150 mm, and the seat height is 420 mm. It is worth noting that the height of the table should depend on the growth of the operator.

The following requirements are also provided for the organization of the workplace of the PC user: The design of the working chair should ensure the maintenance of a rational working posture while working on the PC and allow the posture to be changed in order to reduce the static tension of the neck and shoulder muscles and back to prevent the development of fatigue.

The type of working chair should be selected taking into account the growth of the user, the nature and duration of work with the PC. The working chair should be lifting and swivel, adjustable in height and angle of inclination of the seat and back, as well as the distance of the back from the front edge of the seat, while the adjustment of each parameter should be independent, easy to carry out and have a secure fit.

Occupational safety

A dangerous factor or industrial hazard is a factor whose impact under certain conditions leads to trauma or other sudden, severe deterioration of health of the worker [12].

A harmful factor or industrial health hazard is a factor, the effect of which on a worker under certain conditions leads to a disease or a decrease in working capacity.

4.4.1 Analysis of harmful and dangerous factors that can create object of investigation

The object of investigation is the simulation of OTR and ODR intensity distributions by using Wolfram Mathematica software package. Therefore object of investigation itself cannot cause harmful and dangerous factors.

4.4.2. Analysis of harmful and dangerous factors that can arise at workplace during investigation

The working conditions in the workplace are characterized by the presence of hazardous and harmful factors, which are classified by groups of elements: physical, chemical, biological, psychophysiological. The main elements of the production process that form dangerous and harmful factors are presented in Table 19.

Table 19 – Possible hazardous and harmful factors

Factors (GOST 12.0.003-2015)	Work stages			Legal documents
	Development	Manufacture	Exploitation	
1. Deviation of microclimate indicators	+	+	+	Sanitary rules 2.2.2 / 2.4.1340–03. Sanitary and epidemiological rules and regulations "Hygienic requirements for personal electronic computers and work organization." Sanitary rules 2.2.1 / 2.1.1.1278–03. Hygienic requirements for natural, artificial and combined lighting of residential and
2. Excessive noise		+	+	
3.Increased level of electromagnetic radiation	+	+	+	
4.Insufficient illumination of the working area		+	+	

				public buildings. Sanitary rules 2.2.4 / 2.1.8.562–96. Noise at workplaces, in premises of residential, public buildings and in the construction area. Sanitary rules 2.2.4.548–96. Hygienic requirements for the microclimate of industrial premises.
5. Abnormally high voltage value in the circuit, the closure which may occur through the human body	+	+	+	Sanitary rules GOST 12.1.038-82 SSBT. Electrical safety. Maximum permissible levels of touch voltages and currents.

The following factors effect on person working on a computer:

- physical:
  - temperature and humidity;

- noise;
- static electricity;
- electromagnetic field of low purity;
- illumination;
- presence of radiation;

- psychophysiological:
- psychophysiological dangerous and harmful factors are divided into:
- physical overload (static, dynamic)
- mental stress (mental overstrain, monotony of work, emotional overload).

Deviation of microclimate indicators

The air of the working area (microclimate) is determined by the following parameters: temperature, relative humidity, air speed. The optimum and permissible values of the microclimate characteristics are established in accordance with [13] and are given in Table 20.

Table 20 – Optimal and permissible parameters of the microclimate

Period of the year	Temperature, C	Relative humidity,%	Speed of air movement, m/s
Cold and changing of seasons	23-25	40-60	0.1
Warm	23-25	40	0.1

Excessive noise

Noise and vibration worsen working conditions, have a harmful effect on the human body, namely, the organs of hearing and the whole body through the central nervous system. It result in weakened attention, deteriorated memory, decreased response, and increased number of errors in work. Noise can be generated by operating equipment, air conditioning units, daylight illuminating devices, as well as spread from the outside. When working on a PC, the noise level in the workplace should not exceed 50 dB.

Increased level of electromagnetic radiation

The screen and system blocks produce electromagnetic radiation. Its main part comes from the system unit and the video cable. According to [13], the intensity of the electromagnetic field at a distance of 50 cm around the screen along the electrical component should be no more than:

- in the frequency range 5 Hz - 2 kHz - 25 V / m;
- in the frequency range 2 kHz - 400 kHz - 2.5 V / m.

The magnetic flux density should be no more than:

- in the frequency range 5 Hz - 2 kHz - 250 nT;
- in the frequency range 2 kHz - 400 kHz - 25 nT.

Abnormally high voltage value in the circuit

Depending on the conditions in the room, the risk of electric shock to a person increases or decreases. Do not operate the electronic device in conditions of high humidity (relative air humidity exceeds 75% for a long time), high temperature (more than 35 ° C), the presence of conductive dust, conductive floors and the possibility of simultaneous contact with metal components connected to the ground and the metal casing of electrical equipment. The operator works with electrical devices: a computer (display, system unit, etc.) and peripheral devices. There is a risk of electric shock in the following cases:

- with direct contact with current-carrying parts during computer repair;
- when touched by non-live parts that are under voltage (in case of violation of insulation of current-carrying parts of the computer);
- when touched with the floor, walls that are under voltage;
- short-circuited in high-voltage units: power supply and display unit.

Upper limits for values of contact current and voltage

	Voltage, V	Current, mA
Alternate, 50 Hz	2	0.3
Alternate, 400 Hz	3	0.4
Direct	8	1.0

Insufficient illumination of the working area

Light sources can be both natural and artificial. The natural source of the light in the room is the sun, artificial light are lamps. With long work in low illumination conditions and in violation of other parameters of the illumination, visual perception decreases, myopia, eye disease develops, and headaches appear.

According to the standard, the illumination on the table surface in the area of the working document should be 300-500 lux. Lighting should not create glare on the surface of the monitor. Illumination of the monitor surface should not be more than 300 lux.

The brightness of the lamps of common light in the area with radiation angles from 50 to 90° should be no more than 200 cd/m, the protective angle of the lamps should be at least 40°. The safety factor for lamps of common light should be assumed to be 1.4. The ripple coefficient should not exceed 5%.

4.4.3 Justification of measures to reduce the levels of exposure to hazardous and harmful factors on the researcher

Deviation of microclimate indicators

The measures for improving the air environment in the production room include: the correct organization of ventilation and air conditioning, heating of room. Ventilation can be realized naturally and mechanically. In the room, the following volumes of outside air must be delivered:

- at least 30 m^3 per hour per person for the volume of the room up to 20 m^3 per person;

- natural ventilation is allowed for the volume of the room more than 40 m ^{3} per person and if there is no emission of harmful substances.

The heating system must provide sufficient, constant and uniform heating of the air. Water heating should be used in rooms with increased requirements for clean air.

The parameters of the microclimate in the laboratory regulated by the central heating system, have the following values: humidity 40%, air speed 0.1 m / s, summer temperature 20-25 ° C, in winter 13-15 ° C. Natural ventilation is provided in the laboratory. Air enters and leaves through the cracks, windows, doors. The main disadvantage of such ventilation is that the fresh air enters the room without preliminary cleaning and heating.

Excessive noise

In research audiences, there are various kinds of noises that are generated by both internal and external noise sources. The internal sources of noise are working equipment, personal computer, printer, ventilation system, as well as computer equipment of other engineers in the audience. If the maximum permissible conditions are exceeded, it is sufficient to use sound-absorbing materials in the room (sound-absorbing wall and ceiling cladding, window curtains). To reduce the noise penetrating outside the premises, install seals around the perimeter of the doors and windows.

Increased level of electromagnetic radiation

There are the following ways to protect against EMF:

- increase the distance from the source (the screen should be at least 50 cm from the user);
- the use of pre-screen filters, special screens and other personal protective equipment.

When working with a computer, the ionizing radiation source is a display. Under the influence of ionizing radiation in the body, there may be a violation of normal blood coagulability, an increase in the fragility of blood vessels, a decrease in immunity, etc. The dose of irradiation at a distance of 20 cm to the display is 50 μrem/hr. According to the norms [13], the design of the computer should provide the power of the exposure dose of x-rays at any point at a distance of 0.05 m from the screen no more than 100 μR / h.

Fatigue of the organs of vision can be associated with both insufficient illumination and excessive illumination, as well as with the wrong direction of light.

Abnormally high voltage value in the circuit

Measures to ensure the electrical safety of electrical installations:

- disconnection of voltage from live parts, on which or near to which work will be carried out, and taking measures to ensure the impossibility of applying voltage to the workplace;
- posting of posters indicating the place of work;
- electrical grounding of the housings of all installations through a neutral wire;
- coating of metal surfaces of tools with reliable insulation;
- inaccessibility of current-carrying parts of equipment (the conclusion in the case of electroporating elements, the conclusion in the body of current-carrying parts) [14].

Insufficient illumination of the working area

Desktops should be placed in such a way that the monitors are oriented sideways to the light openings, so that natural light falls mainly on the left.

Also, as a means of protection to minimize the impact of the factor, local lighting should be installed due to insufficient lighting, window openings should be equipped with adjustable devices such as blinds, curtains, external visors, etc.

4.5 Ecological safety

4.5.1 Analysis of the impact of the research object on the environment

The using of radio waves gives to industry great possibilities and finds a wide range of applications. The most known are communications. As energy of radio waves is dissipated with distance effect of irradiation by radio waves was thoroughly study by scientist. There are a series of standards and legal notes to limit power of radio waves sources due harmful effect on biological tissues.

The impact on hydrosphere, atmosphere and lithosphere is a question to debate because of a small number of investigations in this field. Main impact could be only from powerful sources like radiolocation stations.

Mass production of plastic began only 60 years ago. During this time, its output increased 180 times. Recycling takes only 9% of the plastic. Another 12% is burned, and 79% goes to landfills and the environment.

As a result, there is pollution by debris of the lithosphere and hydrosphere. Due to the circulation of currents in the oceans, "garbage islands" are formed. At the same time, plastic not only drifts on the surface, but sinks to the bottom.

In addition to large plastic wastes, there are also wastes due to microplastics. According to international classification, any plastic particle less than 5 mm in length falls into this category. Microplastic is divided into primary and secondary. Primary is most often fibers added to synthetic clothing. When rubbing on a surface or washing, thousands of fibers are separated from it, “hanging” in the air or washed off into the sewer. The second most important source is particles of artificial rubber from tires, which each car leaves 20 grams per 100 km of track. In addition, cars erase markings from roads, which also contain plastic. Secondary microplastic is added to this - “large” debris, broken up into small pieces. As you know, plastic has decomposed for centuries. But it can quickly degrade to tiny parts, while maintaining its molecular structure.

The solutions to the plastic problem today are legislative restrictions on the use of plastic and disposable products, sorting and processing of waste. But they are still not effective solutions to the problem.

4.5.2 Analysis of the environmental impact of the research process

Process of investigation itself in the thesis do not have essential effect on environment. One of hazardous waste is fluorescent lamps. Mercury in fluorescent lamps is a hazardous substance and its improper disposal greatly poisons the environment.

Outdated devices goes to an enterprise that has the right to process wastes. It is possible to isolate precious metals with a purity in the range of 99.95–99.99% from computer components. A closed production cycle consists of the following stages: primary sorting of equipment; the allocation of precious, ferrous and non-ferrous metals and other materials; melting; refining and processing of metals. Thus, there is an effective disposal of computer devices.

4.5.3 Justification of environmental protection measures

Pollution reduction is possible due to the improvement of devices that produces electricity, the use of more economical and efficient technologies, the use of new methods for generating electricity and the introduction of modern methods and methods for cleaning and neutralizing industrial waste. In addition, this problem should be solved by efficient and economical use of electricity by consumers themselves. This is the use of more economical devices, as well as efficient regimes of these devices. This also includes compliance with production discipline in the framework of the proper use of electricity.

Simple conclusion is that it is necessary to strive to reduce energy consumption, to develop and implement systems with low energy consumption. In modern computers, modes with reduced power consumption during long-term idle are widely used.

4.6 Safety in emergency

4.6.1 Analysis of probable emergencies that may occur at the workplace during research

The fire is the most probable emergency in our life. Possible causes of fire:

- malfunction of current-carrying parts of installations;
- work with open electrical equipment;
- short circuits in the power supply;

- non-compliance with fire safety regulations;
- presence of combustible components: documents, doors, tables, cable insulation, etc.

Activities on fire prevention are divided into: organizational, technical, operational and regime.

4.6.2 Substantiation of measures for the prevention of emergencies and the development of procedures in case of emergencies

Organizational measures provide for correct operation of equipment, proper maintenance of buildings and territories, fire instruction for workers and employees, training of production personnel for fire safety rules, issuing instructions, posters, and the existence of an evacuation plan.

The technical measures include compliance with fire regulations, norms for the design of buildings, the installation of electrical wires and equipment, heating, ventilation, lighting, the correct placement of equipment.

The regime measures include the establishment of rules for the organization of work, and compliance with fire-fighting measures. To prevent fire from short circuits, overloads, etc., the following fire safety rules must be observed:

- elimination of the formation of a flammable environment (sealing equipment, control of the air, working and emergency ventilation);
- use in the construction and decoration of buildings of non-combustible or difficultly combustible materials;
- the correct operation of the equipment (proper inclusion of equipment in the electrical supply network, monitoring of heating equipment);
- correct maintenance of buildings and territories (exclusion of the source of ignition - prevention of spontaneous combustion of substances, restriction of fire works);
- training of production personnel in fire safety rules;
- the publication of instructions, posters, the existence of an evacuation plan;

- compliance with fire regulations, norms in the design of buildings, in the organization of electrical wires and equipment, heating, ventilation, lighting;
- the correct placement of equipment;
- well-time preventive inspection, repair and testing of equipment.

In the case of an emergency, it is necessary to:

- inform the management (duty officer);
- call the Emergency Service or the Ministry of Emergency Situations - tel. 112;
- take measures to eliminate the accident in accordance with the instructions.

4.7 Conclusions under social responsibility

In this section about social responsibility the hazardous and harmful factors were revealed. All necessary safety measures and precaution to minimize probability of accidents and traumas during investigation are given.

Possible negative effect on environment were given in compact form describing main ecological problem of using nuclear energy.

It could be stated that with respect to all regulations and standards, investigation itself and object of investigation do not pose special risks to personnel, other equipment and environment.

5 Conclusion

It is shown that covering the half of the lens with opaque screen results in one-lobed structure of the beam image, whereas the lens with no screen produces the beam image with the ring structure. For electron bunches with the size $\Sigma_x > 3$ μm the dependence between FWHM and unknown parameter Σ_x is linear, which allows one to define the transverse bunch size (FWHM ≈ $3\Sigma_x$, if $\Sigma_x \gg 3$ μm). For smaller electron bunch transverse sizes ($\Sigma_x \lesssim 3$ μm) mentioned linear dependence is violated and, for that case, some additional analysis should be carried out, e.g. taking measures of FWHM for different values of radiation wavelength.

The impact of non-ideal focusing conditions (i.e. lens displacement along optical axis) on the shape of OTR PFSs and intensity distributions from the whole electron bunch was studied through the simulation. The dependence between distributions' parameters (FWHM and R_{max}) and the values of positioning errors was determined by fitting original calculated data with specific fitting functions. Obtained results could be used to bring corrections to experimental data or optical system itself.

The dependence that is shown in Figure 23 allows determination of the initial vertical position of incident electron at the moment it crosses horizontal slit. However, to obtain horizontal position of the particle a vertical slit should be applied. Despite the fact that the work only considers a single incident particle its results could be easily extrapolated with a good approximation on the electron beam passing through the slit whose width is greater than the beam size.

Suggested method allows determining two coordinates of the incident electron at a time (unlike the method that involves rectangular slit). Accuracy of both methods suggested here depends on the accuracy in defining the position of distributions' peak intensity values, which is determined by the wavelength of ODR, and, in the cases mentioned above, does not exceed 5%. Intensity distributions observed in the work were calculated on a lens plane, therefore, to make method applicable for real-life cases those distributions should be additionally integrated throughout the lens plane to obtain images on the detector.

List of references

[1] Potylitsyn A., “Image of Optical Diffraction Radiation (Odr) Source and Spatial Resolution of Odr Beam Profile Monitor”, Advanced Radiation Sources and Applications, NATO Science Series, Series II: Mathematics, Physics and Chemistry, 199, ed. Wiedemann H., Springer, 2006, 149–163.

[2] Cole, J., Symes, D., Lopes, N., Wood, J., Poder, K., Alatabi, S., Botchway, S., Foster, P., Gratton, S., Johnson, S., Kamperidis, C., Kononenko, O., Lazzari, M., Palmer, C., Rusby, D., Sanderson, J., Sandholzer, M., Sarri, G., Szoke-Kovacs, Z., & Najmudin, Z. (2018). High-resolution μCT of a mouse embryo using a compact laser-driven X-ray betatron sourceProceedings of the National Academy of Sciences, 115, 201802314.

[3] Wu, Y., Zhu, B., Li, G., Zhang, X., Yu, M., Dong, K., Zhang, T., Yang, Y., Bi, B., Yang, J., Tan, F., Fan, W., Lu, F., Wang, S., Zhao, Q., Zhou, W., Cao, L., & Gu, Y. (2018). Towards high-energy, high-resolution computed tomography via a laser driven micro-spot gamma-ray source Scientific Reports, 8.

[4] X. Artru, R. Chehab, K. Honkavaara, A. Variola. Nucl. Instrum.and Meth.B 145, 160–168 (1998).

[5] Potylitsyn, A., Sukhikh, L., Gusvitskii, T., Kube, G., & Novokshonov, A. (2020). Image of the transverse bunch profile via coherent optical transition radiationPhys. Rev. Accel. Beams, 23, 042804.

[6] A. Potylitsyn, L. Sukhikh, G. Kube, and A. Novokshonov, "Spatial resolution improvement for an optical transition radiation monitor by asymmetric light collection," Opt. Express 26, 30231-30244 (2018).

[7] Потылицын А. П. // Письма в ЖЭТФ. 2016. Т. 103. С. 762.

[8] V.A Verzilov, Transition radiation in the pre-wave zone, Physics Letters A, Volume 273, Issues 1–2, 2000, Pages 135-140, ISSN 0375-9601.

[9] A. Potylitsyn et al. IBIC-19

[10] Proceedings of the 9th International Beam Instrumentation Conference (IBIC-2020), Santos, Brazil. – 2020.

[11] Sukhikh, Leonid & Kube, Gero & Alexander, Potylitsyn. (2017). Simulation of transition radiation based beam imaging from tilted targets. Physical Review Accelerators and Beams. 20. 10.1103/PhysRevAccelBeams.20.032802.

[12] Federal Law "On the Fundamentals of Labor Protection in the Russian Federation" of 17.07.99 № 181 – FZ.

[13] SanPiN 2.2.2 / 2.4.1340-03. Sanitary-epidemiological rules and standards "Hygienic requirements for PC and work organization".

[14] GOST 12.1.038-82 Occupational safety standards system. Electrical safety.

[15] Fire and explosion safety of industrial facilities. GOST R12.1.004-85 Occupational safety standards system. Fire safety.